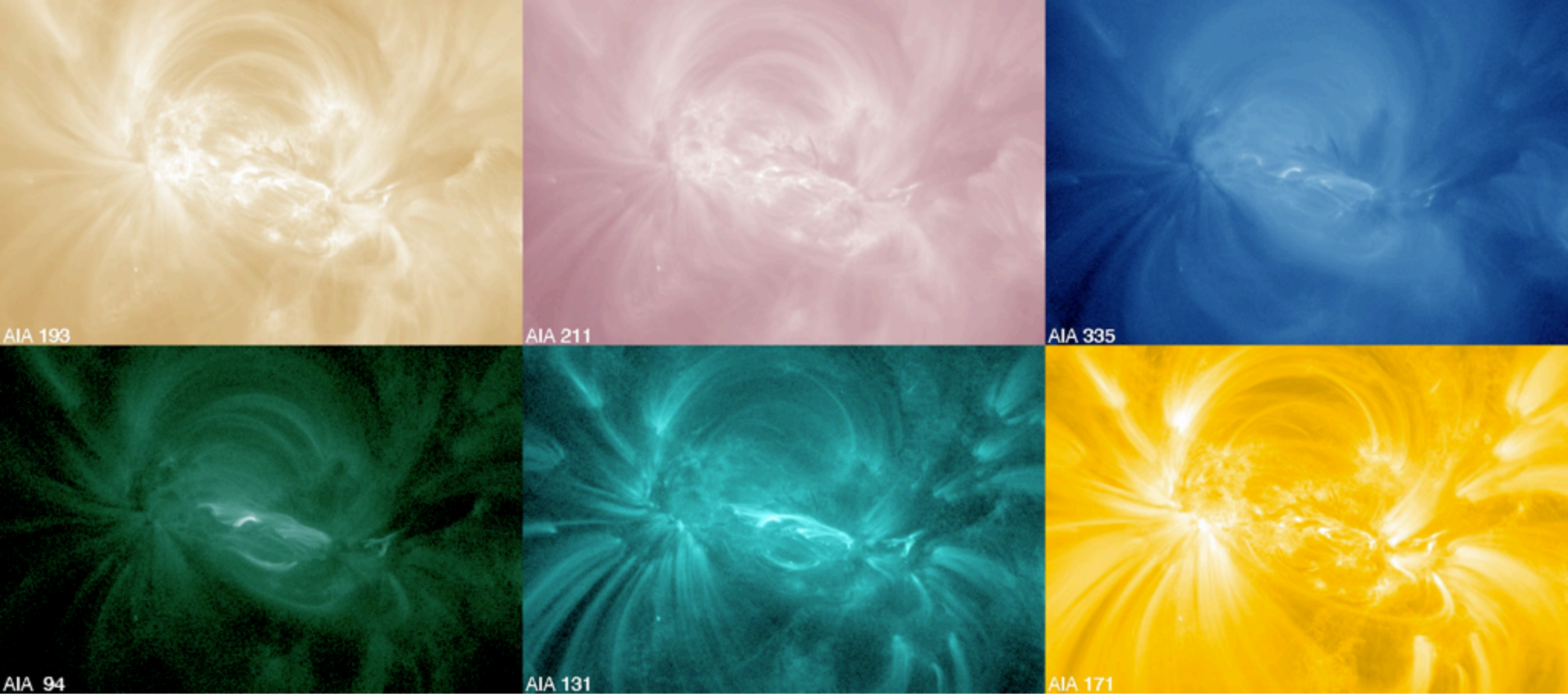

AIA DEM Workshop @ NAOJ

Mark Cheung, LMSAL x NAOJ
cheung@lmsal.com

Schedule

- Monday March 28th
  - 10 am - 12 noon: Lecture (interactive)
  - 1pm onward: Data analysis / lab exercises
- Tuesday March 29th Schedule is flexible
  - BUT 1pm to 2:30pm Shimojo-san ALMA Solar Town Hall
  - Data analysis / lab exercises
  - Show and tell
  - “Office hours”

Outline

1. Aims
2. What do we see in the EUV channels of AIA?
3. Introduction to the problem of Differential Emission Measure (DEM) Inversions
4. Description of sparse solver for AIA data
5. Tutorial on how to use the AIA_SPARSE_EM package
6. Practice exercises
7. Example science problems to tackle

Outline

1. Aims

2. What do we see in the EUV channels of AIA?

3. Introduction to the problem of Differential Emission Measure (DEM) Inversions

4. Description of sparse solver for AIA data

5. Tutorial on how to use the AIA_SPARSE_EM package

6. Practice exercises

7. Example science problems to tackle

Aims

By the end of this workshop, I hope you will have some answers to the following:

- How to find information about AIA data analysis?
- What do SDO/AIA EUV images show?
- What is the differential emission measure (DEM) problem?
- How do we perform DEM inversions on SDO/AIA data?
- How to perform quantitative investigations of the physical evolution of the solar corona?

A taste of what we can do with AIA: Below is a differential emission measure inversion.

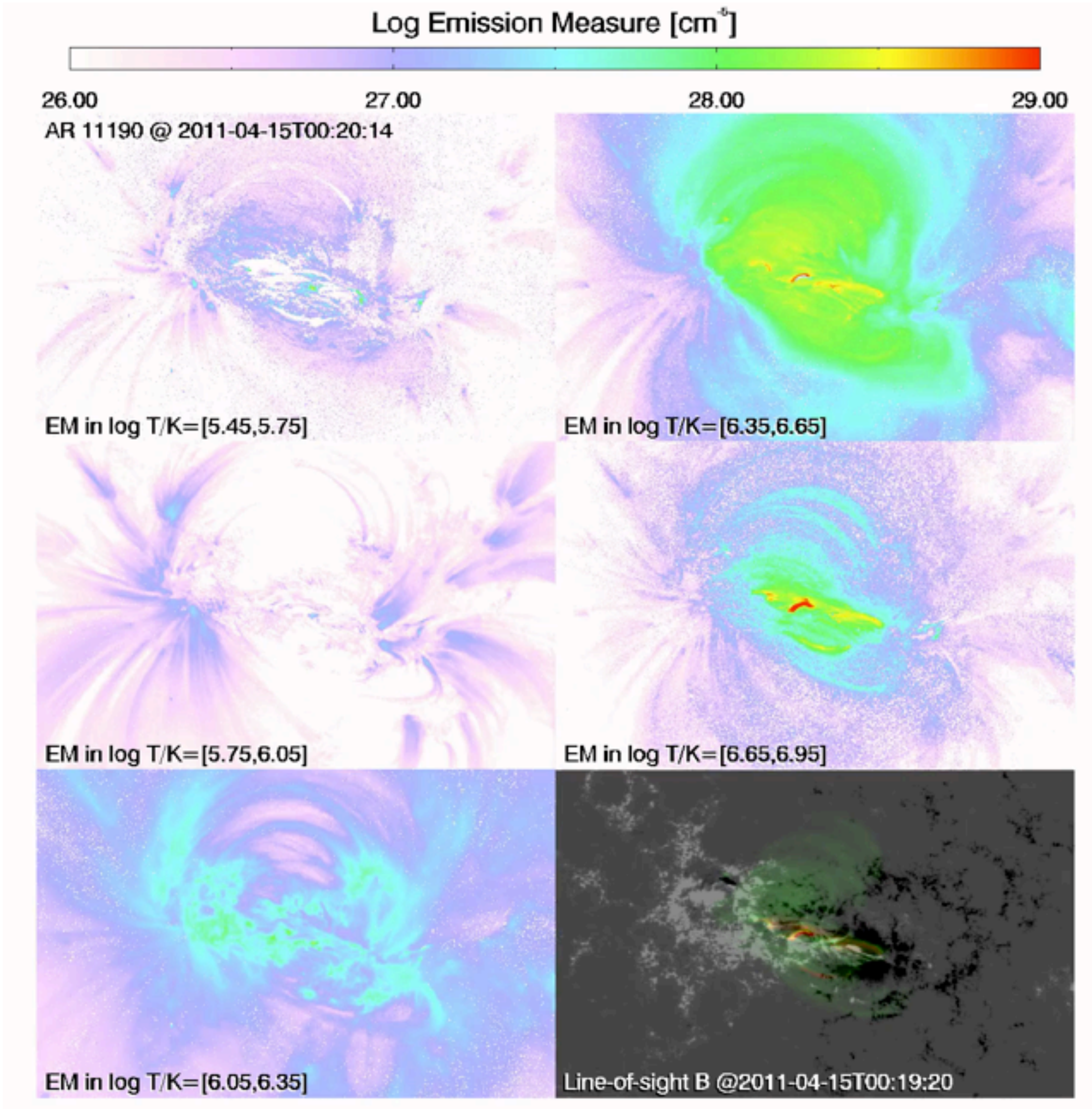

Useful links / documentation

SDO User Guide
http://www.lmsal.com/sdouserguide.html
(Does not yet include how to do DEMs)

AIA DEM package (in beta)
http://tinyurl.com/aiadem

Documentation about AIA
https://www.lmsal.com/sdodocs/
- AIA Instrument Paper (Lemen et al. 2012)
- Initial Calibration of AIA (Boerner et al. 2012)

CHIANTI User Guide
$SSW/packages/chianti/doc/cug.pdf

SDO User Guide

http://www.lmsal.com/sdouserguide.html

Outline

1. Aims

2. What do we see in the EUV channels of AIA?

3. Introduction to the problem of Differential Emission Measure (DEM) Inversions

4. Description of sparse solver for AIA data

5. Tutorial on how to use the AIA_SPARSE_EM package

6. Practice exercises

7. Example science problems to tackle

What do we see in AIA/EUV images?

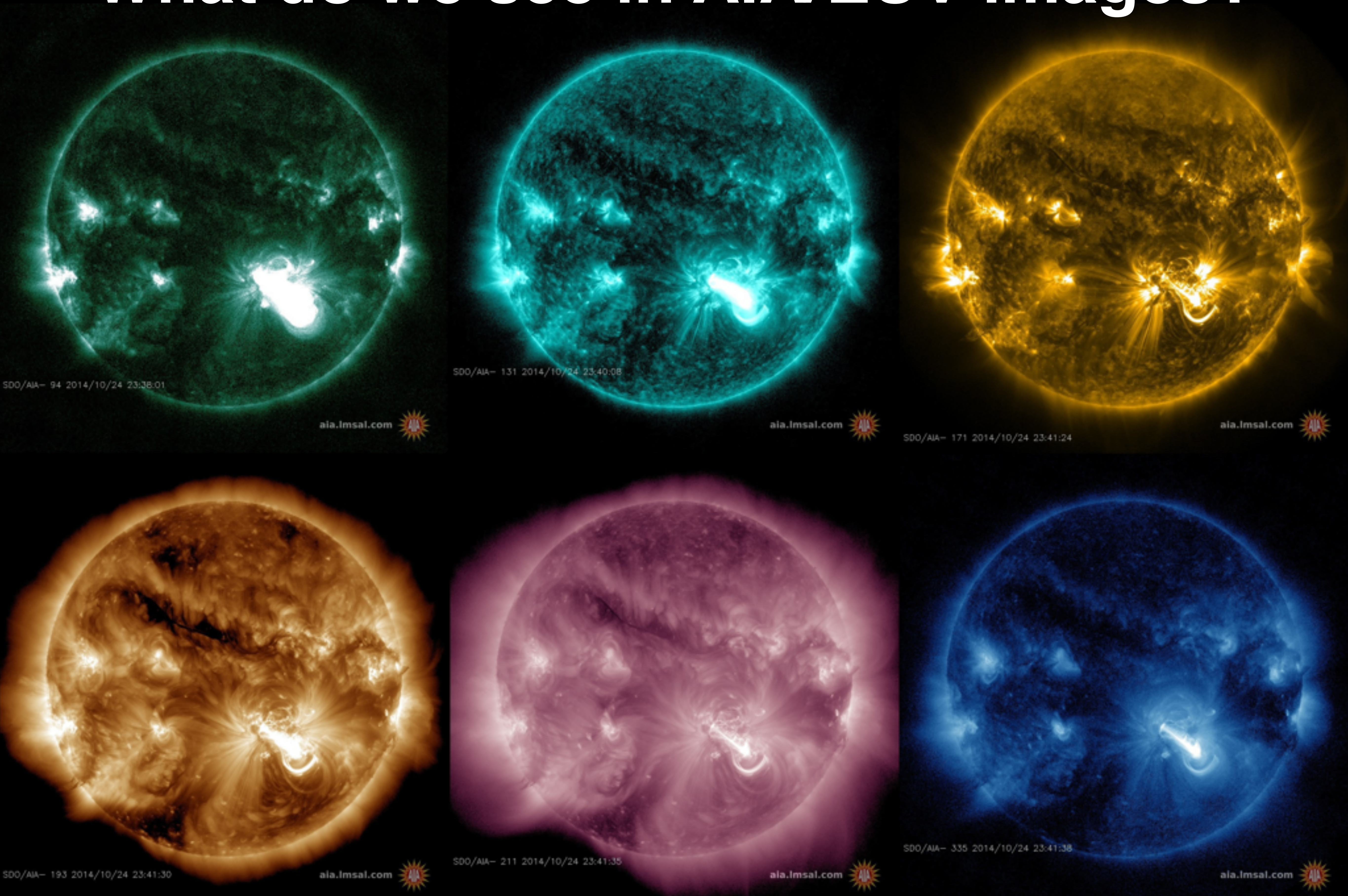

What do EUV images from SDO/AIA show?

```
;       Name: aia_get_response
;
;       Purpose: return SDO/AIA instrument response data structures
;
;       Input Parameters:
;
;       Output:
;               function returns AIA wavelength response, spectral model, or temperature response
;               Descriptions of the structures returned by this routine are available via:
;                       http://sohowww.nascom.nasa.gov/solarsoft/sdo/aia/response/README.txt
;
;       Calling Examples:
;               IDL> effarea=aia_get_response(/area, /dn)        ;  return per wavelength effective area
;               IDL> effarea=aia_get_response(/area,/full,/dn)   ;  same with component details (filter/ccd...)
;               IDL> emiss=aia_get_response(/emiss, /full)       ;  return default CHIANTI model with line list
;               IDL> tresp=aia_get_response(/temp,/dn,/evenorm) ; return temperature response including
;                                                                ; constant scale factors to give good
;                                                                ; overall agreement with SDO/EVE
;
```

<u>See section 6.5 of SDO User Guide for extensive explanation.</u>

AIA Temperature Response Functions

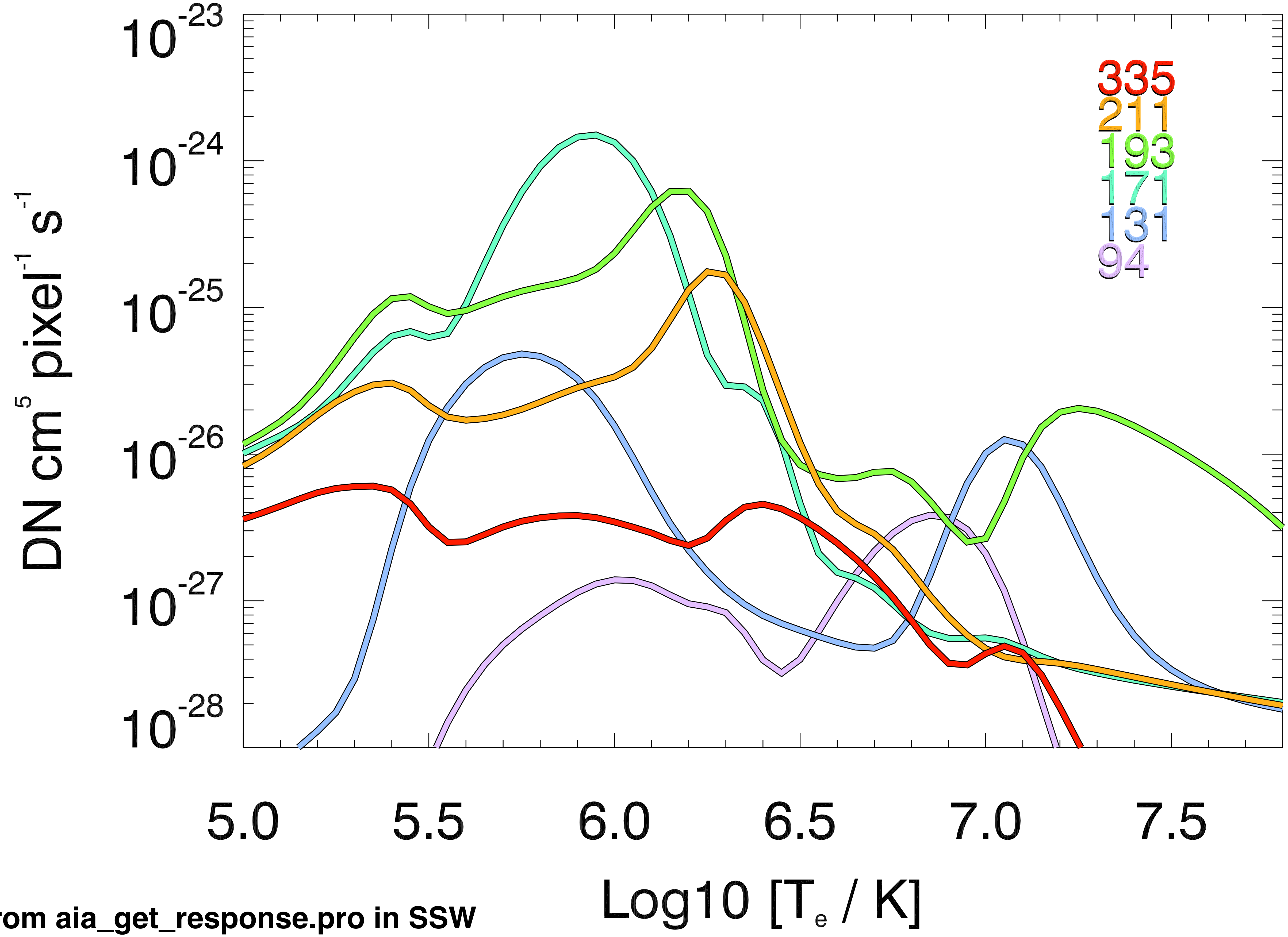

From aia_get_response.pro in SSW

Table 1. Predicted AIA count rates.

From O'Dwyer et al. 2010

	Ion	λ Å	T_p^a K	Fraction of total emission CH	QS	AR	FL
94 Å	Mg VIII	94.07	5.9	0.03	-	-	-
	Fe XX	93.78	7.0	-	-	-	0.10
	Fe XVIII	93.93	6.85	-	-	0.74	0.85
	Fe X	94.01	6.05	0.63	0.72	0.05	-
	Fe VIII	93.47	5.6	0.04	-	-	-
	Fe VIII	93.62	5.6	0.05	-	-	-
	Cont.			0.11	0.12	0.17	-
131 Å	O VI	129.87	5.45	0.04	0.05	-	-
	Fe XXIII	132.91	7.15	-	-	-	0.07
	Fe XXI	128.75	7.05	-	-	-	0.83
	Fe VIII	130.94	5.6	0.30	0.25	0.09	-
	Fe VIII	131.24	5.6	0.39	0.33	0.13	-
	Cont.			0.11	0.20	0.54	0.04
171 Å	Ni XIV	171.37	6.35	-	-	0.04	-
	Fe X	174.53	6.05	-	0.03	-	-
	Fe IX	171.07	5.85	0.95	0.92	0.80	0.54
	Cont.			-	-	-	0.23
193 Å	O V	192.90	5.35	0.03	-	-	-
	Ca XVII	192.85	6.75	-	-	-	0.08
	Ca XIV	193.87	6.55	-	-	0.04	-
	Fe XXIV	192.03	7.25	-	-	-	0.81
	Fe XII	195.12	6.2	0.08	0.18	0.17	-
	Fe XII	193.51	6.2	0.09	0.19	0.17	-
	Fe XII	192.39	6.2	0.04	0.09	0.08	-
	Fe XI	188.23	6.15	0.09	0.10	0.04	-
	Fe XI	192.83	6.15	0.05	0.06	-	-
	Fe XI	188.30	6.15	0.04	0.04	-	-
	Fe X	190.04	6.05	0.06	0.04	-	-
	Fe IX	189.94	5.85	0.06	-	-	-
	Fe IX	188.50	5.85	0.07	-	-	-
	Cont.			-	-	0.05	0.04
211 Å	Cr IX	210.61	5.95	0.07	-	-	-
	Ca XVI	208.60	6.7	-	-	-	0.09
	Fe XVII	204.67	6.6	-	-	-	0.07
	Fe XIV	211.32	6.3	-	0.13	0.39	0.12
	Fe XIII	202.04	6.25	-	0.05	-	-
	Fe XIII	203.83	6.25	-	-	0.07	-
	Fe XIII	209.62	6.25	-	0.05	0.05	-
	Fe XI	209.78	6.15	0.11	0.12	-	-
	Fe X	207.45	6.05	0.05	0.03	-	-
	Ni XI	207.92	6.1	0.03	-	-	-
	Cont.			0.08	0.04	0.07	0.41
304 Å	He II	303.786	4.7	0.33	0.32	0.27	0.29
	He II	303.781	4.7	0.66	0.65	0.54	0.58
	Ca XVIII	302.19	6.85	-	-	-	0.05
	Si XI	303.33	6.2	-	-	0.11	-
	Cont.			-	-	-	-
335 Å	Al X	332.79	6.1	0.05	0.11	-	-
	Mg VIII	335.23	5.9	0.11	0.06	-	-
	Mg VIII	338.98	5.9	0.11	0.06	-	-
	Si IX	341.95	6.05	0.03	0.03	-	-
	Si VIII	319.84	5.95	0.04	-	-	-
	Fe XVI	335.41	6.45	-	-	0.86	0.81
	Fe XIV	334.18	6.3	-	0.04	0.04	-
	Fe X	184.54	6.05	0.13	0.15	-	-
	Cont.			0.08	0.05	-	0.06

Outline

1. Aims
2. What do we see in the EUV channels of AIA?
3. Introduction to the problem of Differential Emission Measure (DEM) Inversions
4. Description of sparse solver for AIA data
5. Tutorial on how to use the AIA_SPARSE_EM package
6. Practice exercises
7. Example science problems to tackle

Statement of the Problem

The Atmospheric Imaging Assembly (AIA, Lemen et al. 2012; Boerner et al. 2012) instrument onboard NASA's Solar Dynamics Observatory (SDO, Pesnell et al. 2012) is a suite of four normal-incidence reflecting telescopes that image the Sun in seven EUV channels, two UV channels and one visible wavelength channel.

The aim of this and many other studies is to extract thermal information about the Sun's optically thin corona using the EUV observations. The calibrated (i.e. dark-subtracted, flat-fielded and exposure time normalized) count rate y_i in the i-th EUV channel is related to the thermal distribution of coronal plasma by:

$$y_i = \int_0^\infty K_i(T)\ \mathrm{DEM}(T) dT,$$

where $K_i(T)$ is the temperature response function (see next slide):

Statement of the Problem

and $$\mathrm{DEM}(T)dT = \int_0^\infty n_e^2(T)dz,$$

where DEM(T) is the differential emission measure (in units of $cm^{-5}\ K^{-1}$) of plasma along the line-of-sight. $n_e(T)$ is the electron number density of plasma at temperature T. The challenge is to solve for DEM(T) given a set of EUV measurements **y**.

Let the temperature range be divided into n neighboring bins, so that:

$$y_i = \sum_{j=1}^{n} \int_{T_j}^{T_j+\Delta T_j} K_i(T)\mathrm{DEM}(T)dT,$$

where the j-th temperature bin has range $T \in [T_j, T_j+\Delta T_j)$. Assuming that $K_i(T)$ is piecewise constant in each temperature bin, we have:

$$y_i = \sum_{j=1}^{n} K_{ij}\mathrm{EM}_j, \text{where } \mathrm{EM}_j = \int_{T_j}^{T_j+\Delta T_j} \mathrm{DEM}(T)dT.$$

Statement of the Problem: y = Kx

$$y_i = \sum_{j=1}^{n} K_{ij}\mathrm{EM}_j, \text{ where } \mathrm{EM}_j = \int_{T_j}^{T_j+\Delta T_j} \mathrm{DEM}(T)dT.$$

The above is a matrix equation of the form **y** = K**x,** where

- K is an m x n response matrix*, with each row corresponding to the temperature response function of one AIA channel
- **y** is an m-tuple corresponding of AIA count (rates), and
- **x** is an n-tuple with components EM_j.

The He II line in the 304 Å channel is not well-modeled by CHIANTI (Warren, 2005, ApJ 157, 147) so it is usually not used for DEM analysis. So m = 6 for AIA. Usually we want more than 6 temperature bins. **For m < n, the matrix equation y = Kx represents an underdetermined system.**

*Matrix elements depends on basis functions used for computing the integral

Usual Approach: χ-squared Minimization

<u>**Function to minimize:**</u> **$| y - Kx |^2$ or $|(y - Kx)/\sigma|^2$**

Basically, minimize difference between observed and predicted counts. The benefits of a least-squares approach is that it leads to Euler-Lagrange equations that can be used to seek (global or local) minima.

For an overdetermined system, we know no single model will fit all the data. So χ-squared minimization is ideal. However, **for underdetermined systems such an approach can be subject to the perils of overfitting.**

Usual way to get around this:

Parameterization: e.g. Guennou et al (2012a,b), xrt_dem_iterative2.pro (M. Weber in SSW, see also Cheng et al 2012)

Regularization: e.g. Hannah & Kontar (2012), Plowman et al. (2013)

Outline

1. Aims

2. What do we see in the EUV channels of AIA?

3. Introduction to the problem of Differential Emission Measure (DEM) Inversions

4. Description of sparse solver for AIA data

5. Tutorial on how to use the AIA_SPARSE_EM package

6. Practice exercises

7. Example science problems to tackle

Cheung et al. 2015: The Sparse Solution

We address the inverse problem using an approach different than chi-squared minimization. The set of solutions satisfying the underdetermined matrix equation **y** = K**x** lies in an affine subspace of $\mathbf{R}^n$. We pick the solution $\mathbf{x}^{\#}$ within this subspace such that:

$$\text{minimize} \sum_{j}^{n} \mathrm{x}_j \text{ subject to } \mathcal{K}\vec{x} = \vec{y},\ \vec{x} \geq 0.$$

The linear program above finds a solution that minimizes the L1-norm of the solution vector (c.f. Candes 2006). This is not chi-squared minimization.

If K is the response function sampled by Dirac Delta functions at specific temperatures, this is equivalent to minimizing the total EM. If other basis functions are used, there is no simple corresponding physical interpretation.

The Sparse Solution

We are unaware of physical principles pertaining to coronal plasma that motivate the optimization problem posed above. However, this choice has some important benefits:

1) It does not overfit (consistent with the principle of parsimony, i.e. Ockham's Razor).
2) It ensures positivity of the solution (if solutions exist).
3) It is an L1-norm minimization problem, so we can use standard techniques from compressed sensing (c.f. Candes & Tao 2006).

   BTW the L1-norm of a vector x = Σ $|x_i|$

4) Speed: $O(10^4)$ solutions / sec with single IDL thread.

Handling noise

In practice, measurement uncertainties imply that the equality **y** = K**x** may not be satisfied. So our method solves the followed modified linear program:

$$\text{minimize} \sum_j^n \mathrm{x}_j \text{ subject to } \mathcal{K}\vec{x} \leq \vec{y} + \vec{\eta},$$
$$\vec{x} \geq 0,\ \ \mathcal{K}\vec{x} \geq \max(\vec{y} - \vec{\eta}, 0).$$

The vector **η** is a measure of the uncertainty in the count rate and provides tolerance for the predicted counts (K**x)** to deviate from the observed values (**y**). To enforce positive counts the lower bound is set to max(**y-η**, 0).

χ-squared minimization

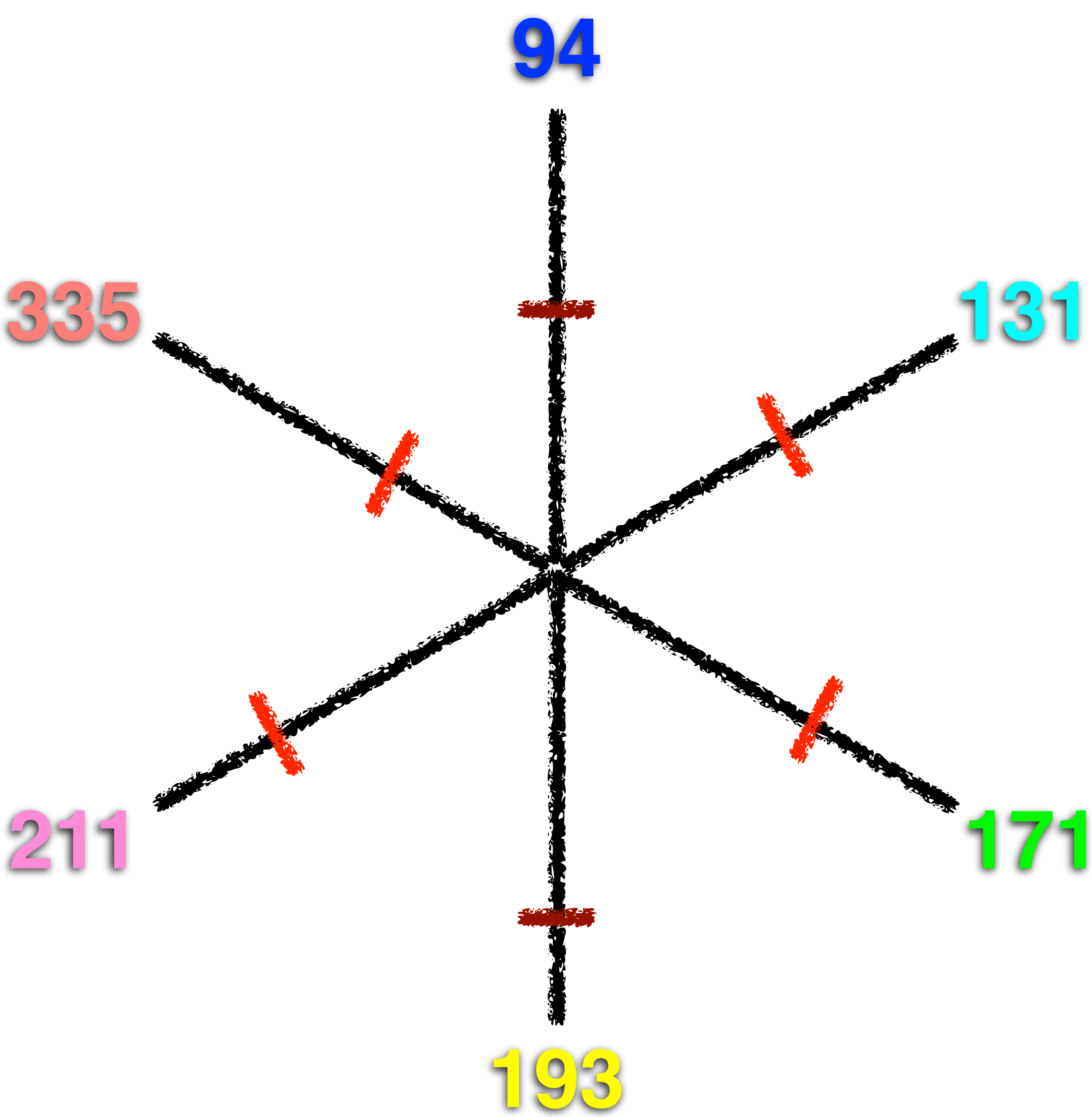

vs.

Sparse inversion

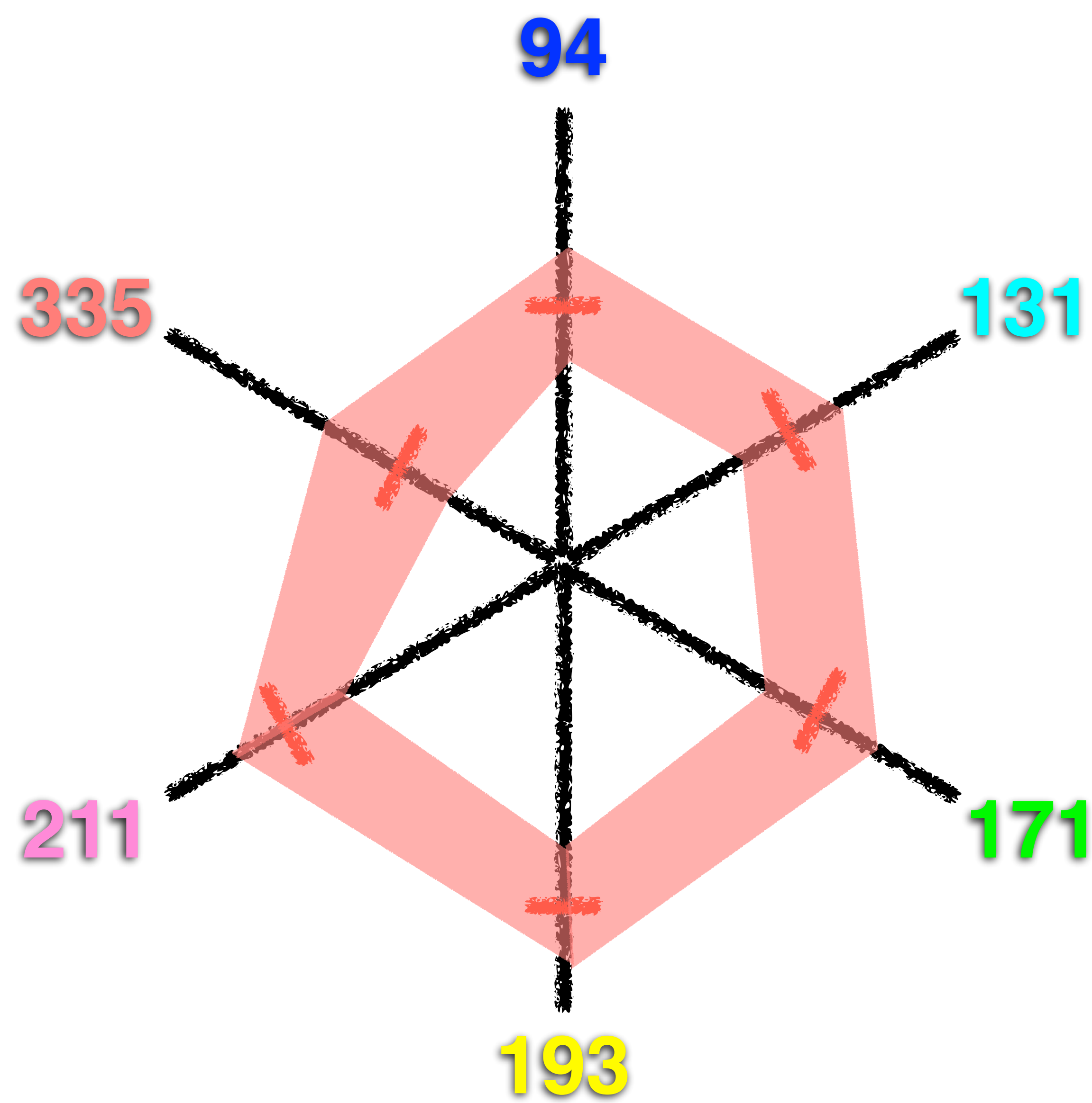

Crossmarks are observed counts

Subspace of allowed solutions in our method

Basis Functions for DEM

Let $i = 1, 2, ..., m$ denote the index over a set of wavelength band channels and/or line spectra. Let the DEM function be written in terms of a set of positive semidefinite basis functions $\{b_j(\log T) \geq 0 \mid k = 1, 2, ..., l\}$, viz.

$$\mathrm{DEM}(\log T) = \sum_{k=1}^{l} b_k(\log T) x_k, \tag{A1}$$

with quadrature coefficients $x_k \geq 0$. Approximating the integrals in equation (1) as sums in $\log T$ space, we have

$$y_i = \sum_{j=1}^{n} \sum_{k=1}^{l} K_{ij} B_{jk} x_k \Delta \log T, \tag{A2}$$

where $j = 1, 2, ..., n$ is the index over temperature bins, $K_{ij} = K_i(\log T_j)$ and $B_{jk} = b_k(\log T_j)$. The response matrix $\mathbf{K} = (K_{ij})$ has dimensions $m \times n$. The basis matrix $\mathbf{B} = (B_{jk})$ has dimensions $n \times l$, with the k-th column vector corresponding to the k-th basis function $b_k(\log T_j)$. Defining the *dictionary matrix* $\boxed{\mathbf{D} = \mathbf{KB}}$, the set of integral equations (1) can be written in matrix form:

In practice we solve this ➜

$$\boxed{\vec{y} = \mathbf{D}\vec{x},} \tag{A3}$$

where the sought-after solution vector $\vec{x}$ is an l-tuple with components $x_k \Delta \log T$ $(k = 1, 2, ..., l)$. When the number of basis functions exceeds the number of image channels (i.e. $l > m$), the linear system Eq. (A3) is underdetermined.

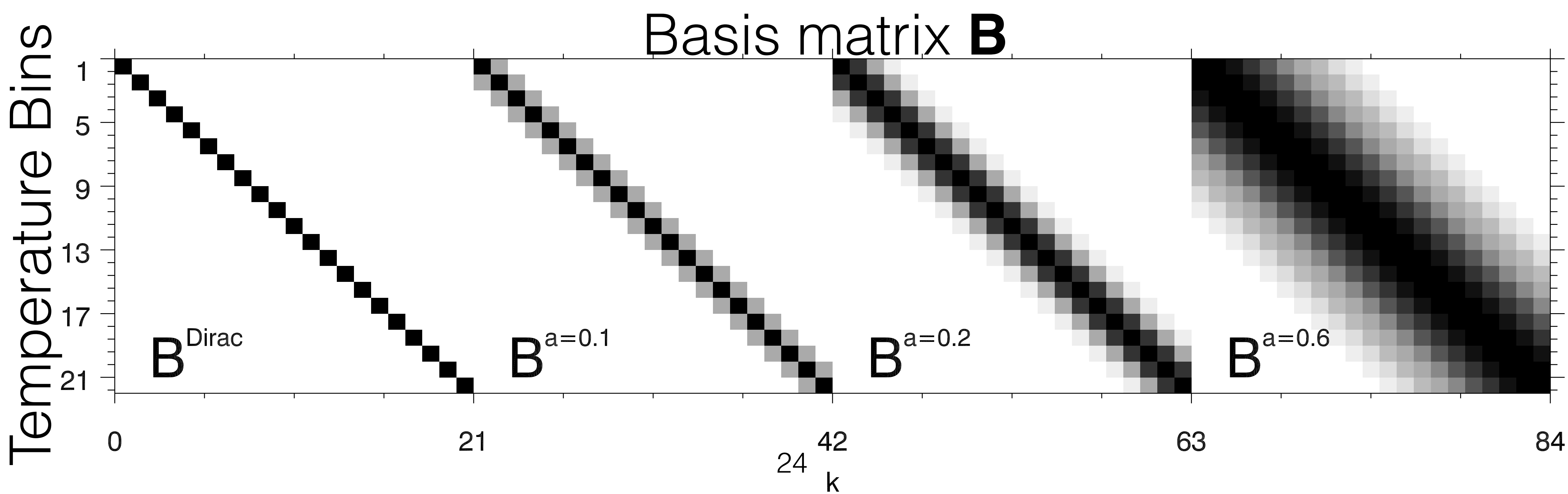

Geometrical Interpretation of Problem

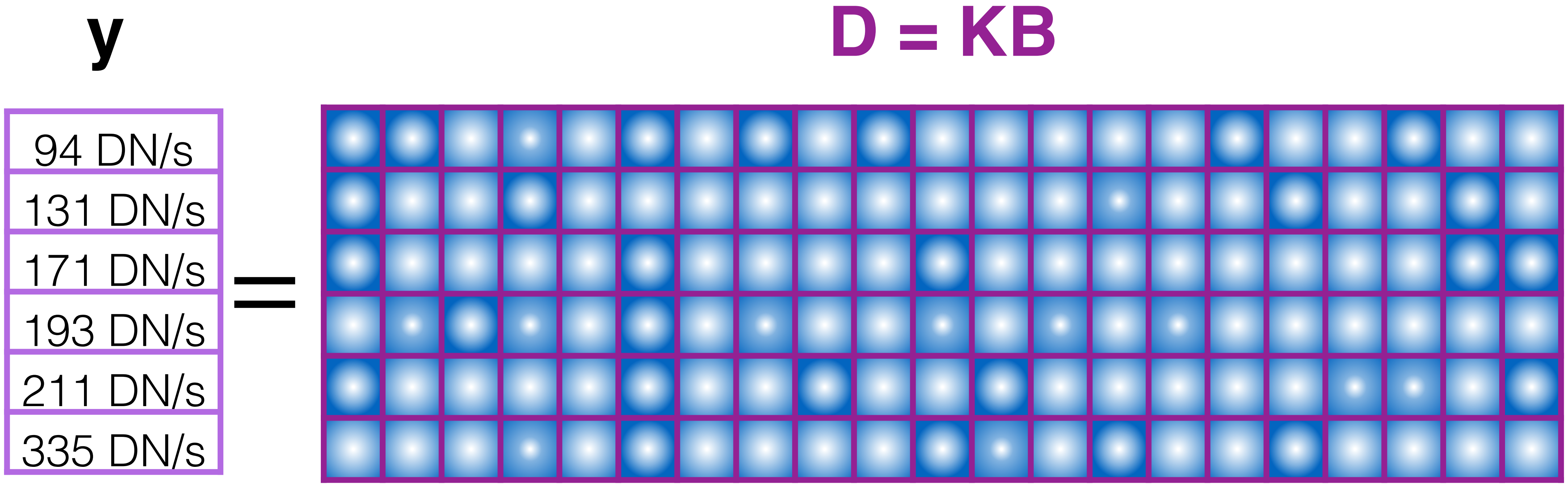

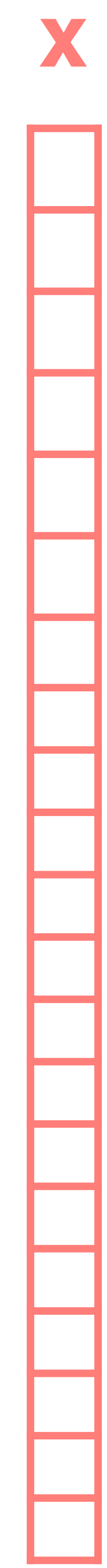

We seek to build a column vector **y** by linear combinations of columns of the matrix **D=KB**. x_j are the coefficients of the linear combination. More columns of **KB** from which to chose than components of **y**

=> underdetermined problem.

Do “basis pursuit” by minimizing L1 norm of x.

Application to real AIA data

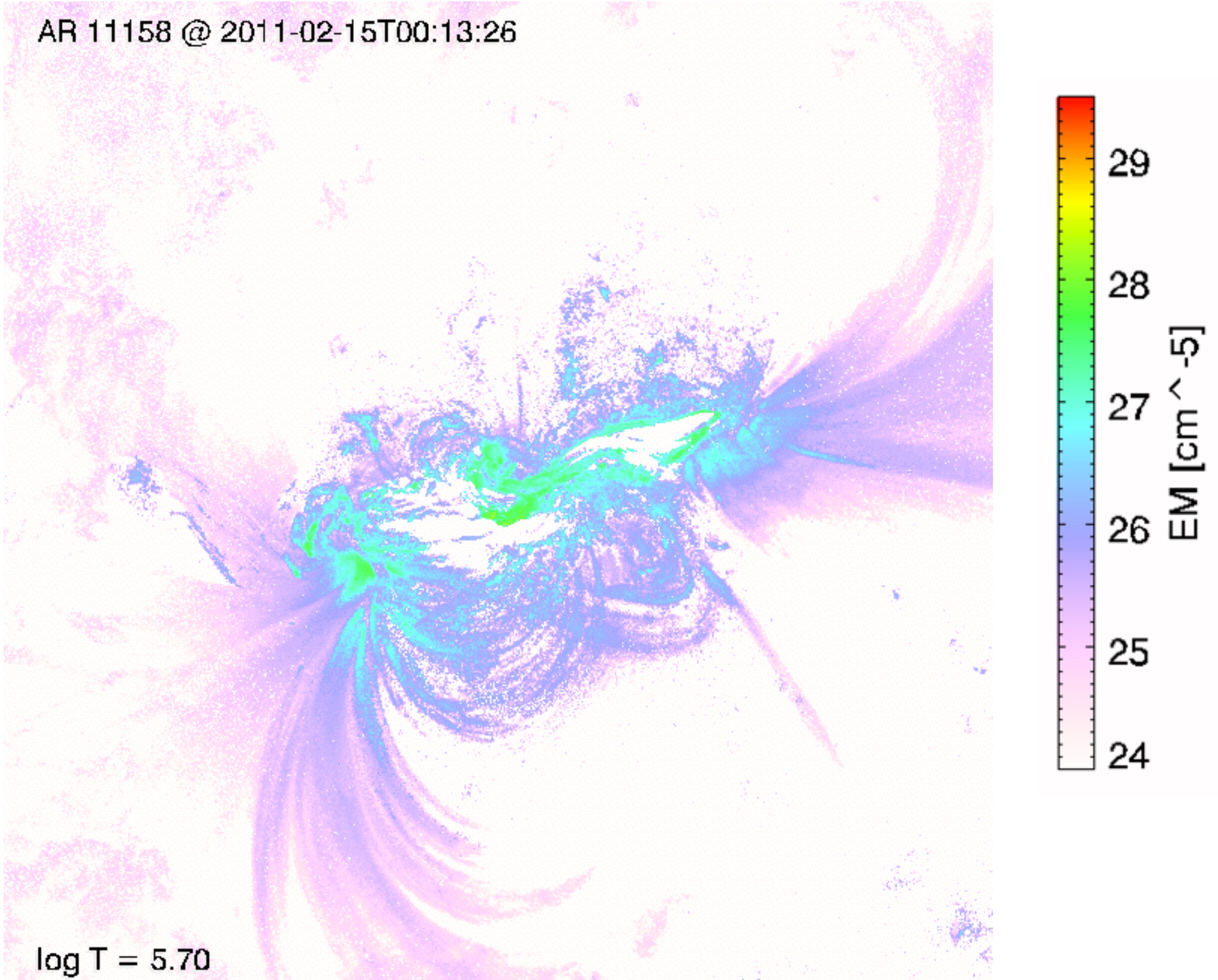

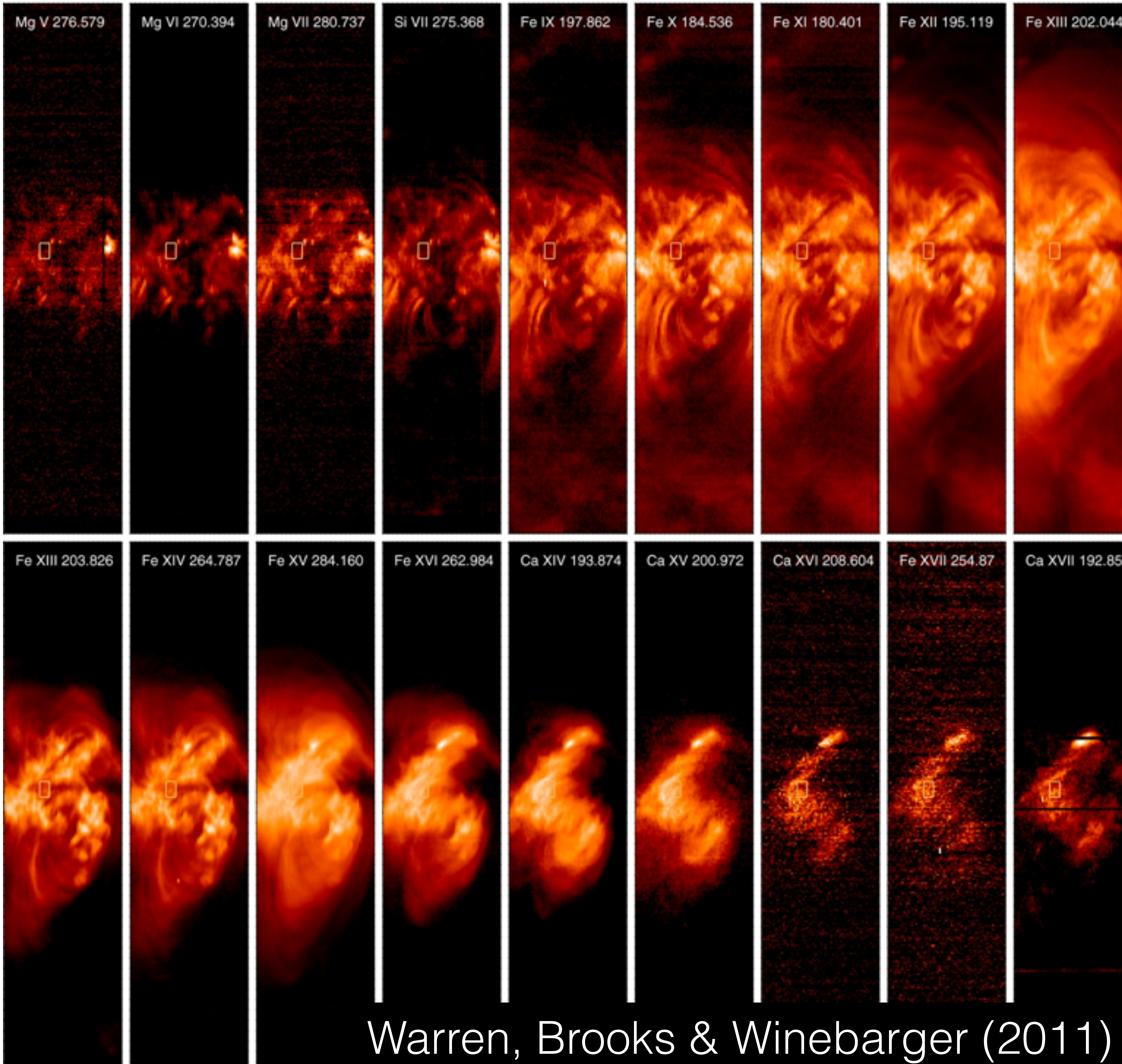

Warren, Brooks & Winebarger (2011)

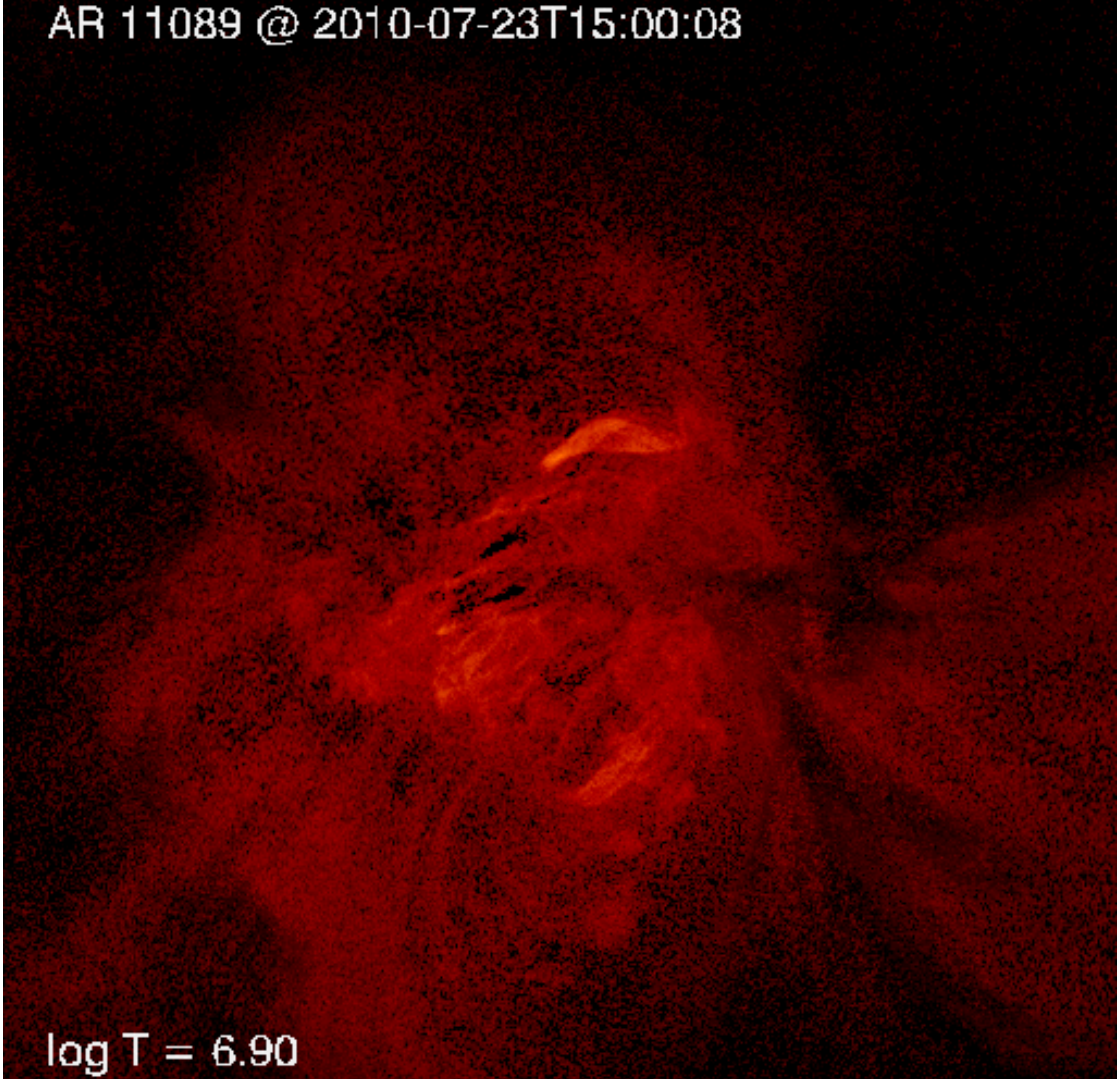
AR 11089 @ 2010-07-23T15:00:08
log T = 6.90

Side benefit: Image Denoising

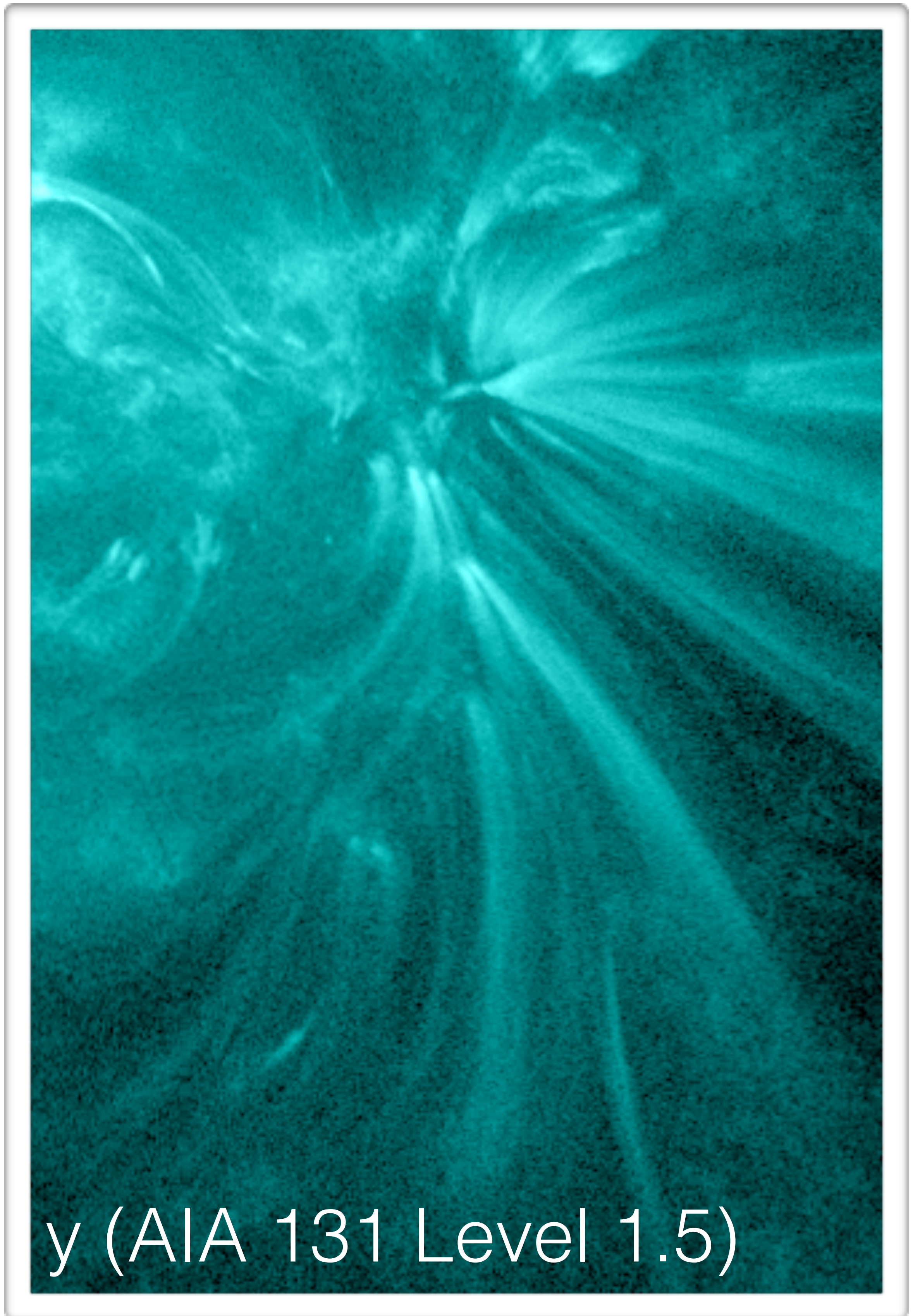

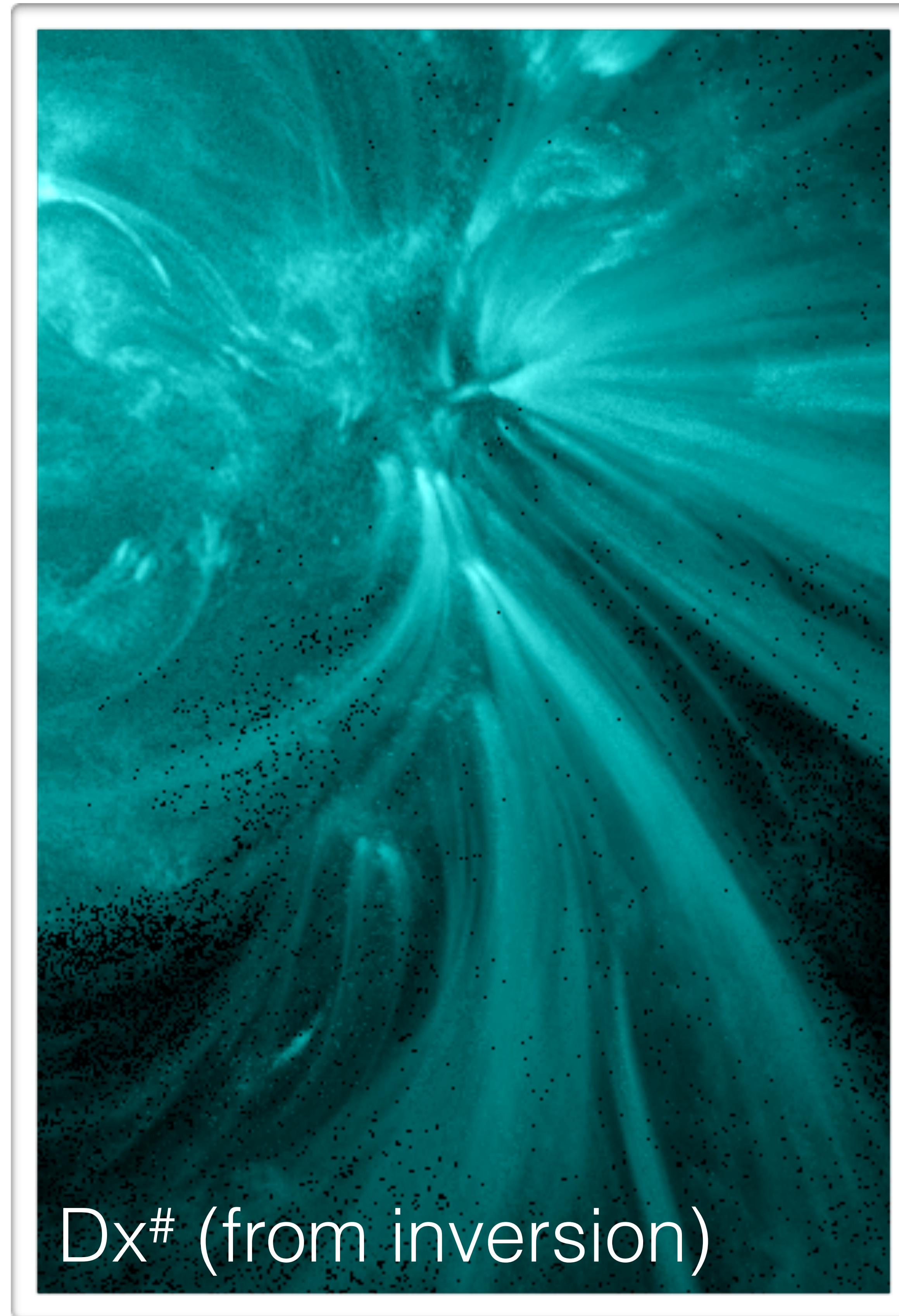

Outline

1. Aims

2. What do we see in the EUV channels of AIA?

3. Introduction to the problem of Differential Emission Measure (DEM) Inversions

4. Description of sparse solver for AIA data

5. Tutorial on how to use the AIA_SPARSE_EM package

6. Practice exercises

7. Example science problems to tackle

How to use the Sparse DEM code

http://tinyurl.com/aiadem

- Instructions in the readme file
- Download *genx files, which contain sample AIA 6-channel data.
- Download aia_sparse_em_init.pro & exercise1.pro

➡ .compile aia_sparse_em_init

➡ .r exercise1 ; Example of DEM inversion

➡ .r exercise2 ; Example of DEM sensitivity to noise

```
; Author: Mark Cheung
; Purpose: Sample script for running sparse DEM inversion (see Cheung
; et al. 2015) for details.
; Revision history: 2015-10-20 First version
;                   2015-10-23 Added note about lgT axis

files = file_list('.','*genx')
aiadatafile = files[0]
; Restore some prepared AIA level 1.5 data (i.e. already been aia_preped)
restgen, file=aiadatafile, struct=s

; Initialize solver.
; This step builds up the response functions (which are
; time-dependent) and the basis functions.
; If running inversions over a set of data spanning over a few hours
; or even days, it is not necessary to re-initialize

;IF (0) THEN BEGIN
; As discussed in the Appendix of Cheung et al. (2015), the inversion
; can push some EM into temperature bins if the lgT axis goes below
; logT ~ 5.7 (see Fig. 18). It is suggested the user check the
; dependence of the solution by varying lgTmin.
lgTmin = 5.7   ; minimum for lgT axis for inversion
dlgT   = 0.1   ; width of lgT bin
nlgT   = 21    ; number of lgT bins
aia_sparse_em_init, timedepend = s.oindex[0].date_obs, /evenorm, $
      use_lgtaxis=findgen(nlgT)*dlgT+lgTmin
lgtaxis = aia_sparse_em_lgtaxis()
; ENDIF
```

```
; We will use the data in s.img to invert. s.img is a stack of level
; 1.5, exposure time normalized AIA pixel values.
exptimestr = '['+strjoin(string(s.oindex.exptime,format='(F8.5)'),',')+']'

; This defines the tolerance function for the inversion.
; y denotes the values in DN/s/pixel (i.e. level 1.5, exposure time
; normalized)

; aia_bp_estimate_error gives the estimated uncertainty for a given
; DN / pixel for a given AIA channel. Since y contains DN/pixel/s,
; we have to multiply by exposure time first to pass
; aia_bp_estimate_error. Then we will divide the output of
; aia_bp_estimate_error by the exposure time again.
; If one wants to include uncertainties in atomic data, suggest to add
; the /temp keyword to aia_bp_estimate_error()
tolfunc = 'aia_bp_estimate_error(y*'+exptimestr+', [94,131,171,193,211,335], $
          num_images=‘+strtrim(string(s.binning^2,format='(I4)'),2)+')/'+exptimestr

; Do DEM solve.
; Note!!! The solver assumes the third dimension is arranged according to
[94,131,171,193,211,335]
aia_sparse_em_solve, s.img, tolfunc=tolfunc, tolfac=1.4, oem=emcube, status=status,
coeff=coeff
```

Output of exercise1.pro

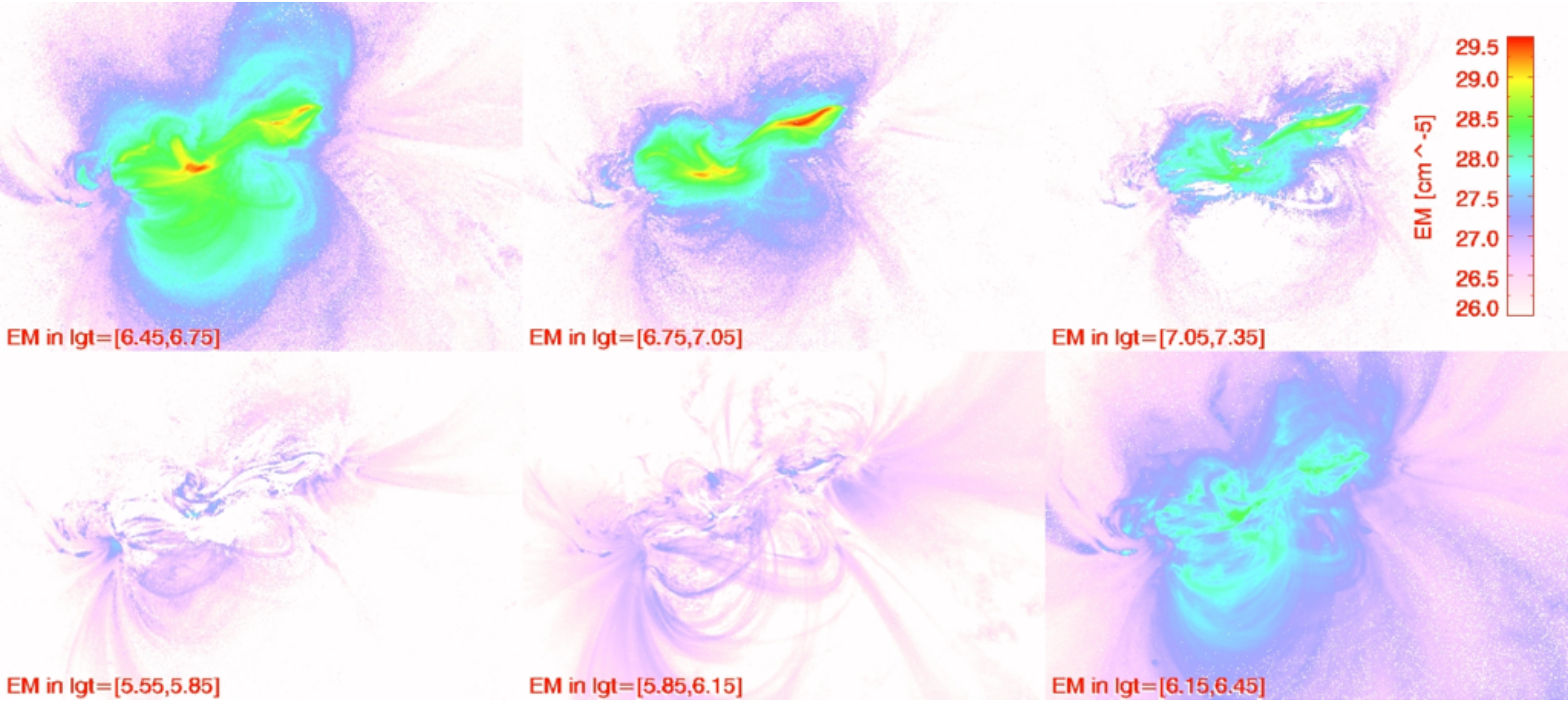

status[Nx, Ny] - Indicating where a DEM solution was found, 0 is yes

coeff[Nx, Ny, 84] - Coefficients of basis functions used to express DEM; i.e. the x in equation y = **KB**x.

emcube[Nx, Ny, 21] - DEM solution. i.e. **B**x.

Interactively inspect DEM profiles

- aia_sparse_dem_inspect, coeff, emcube, status, /ylog

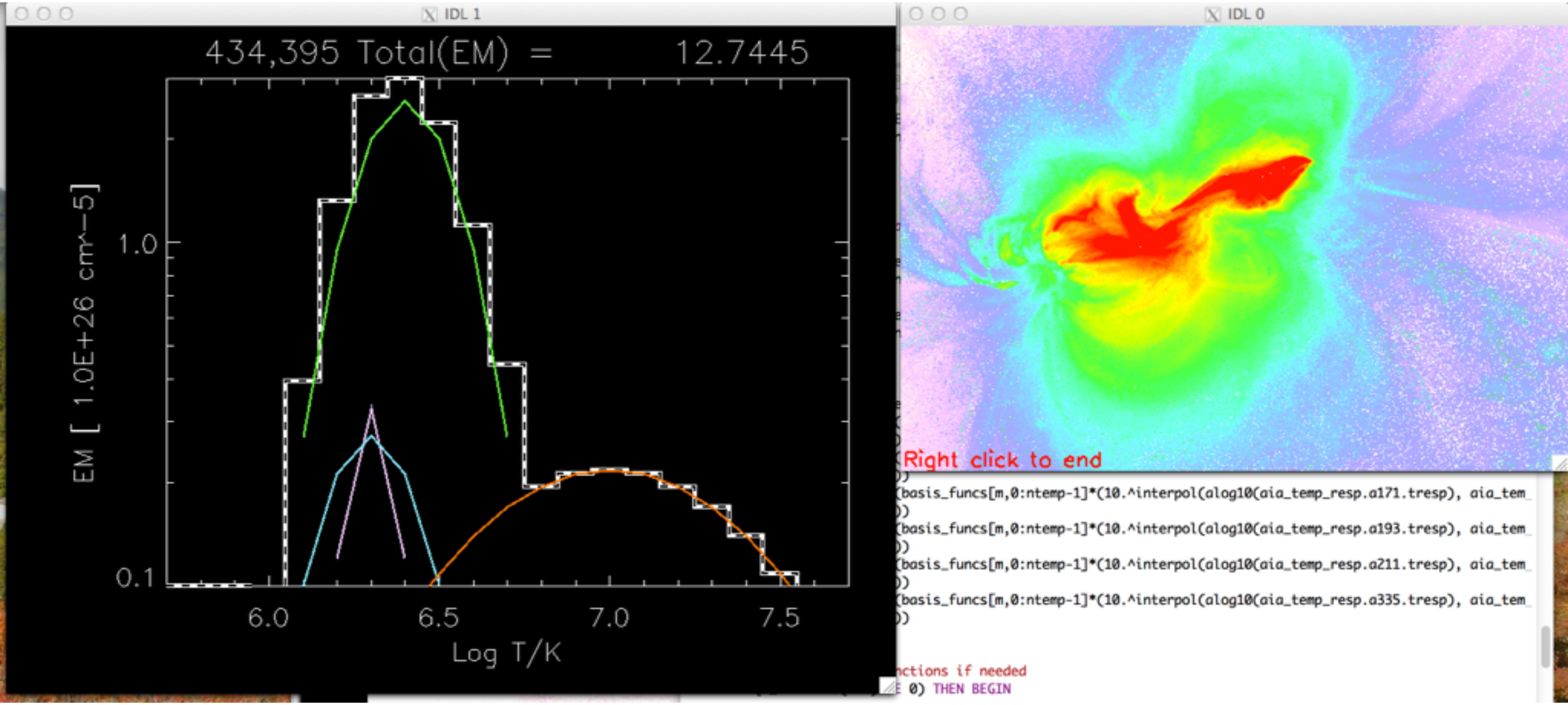

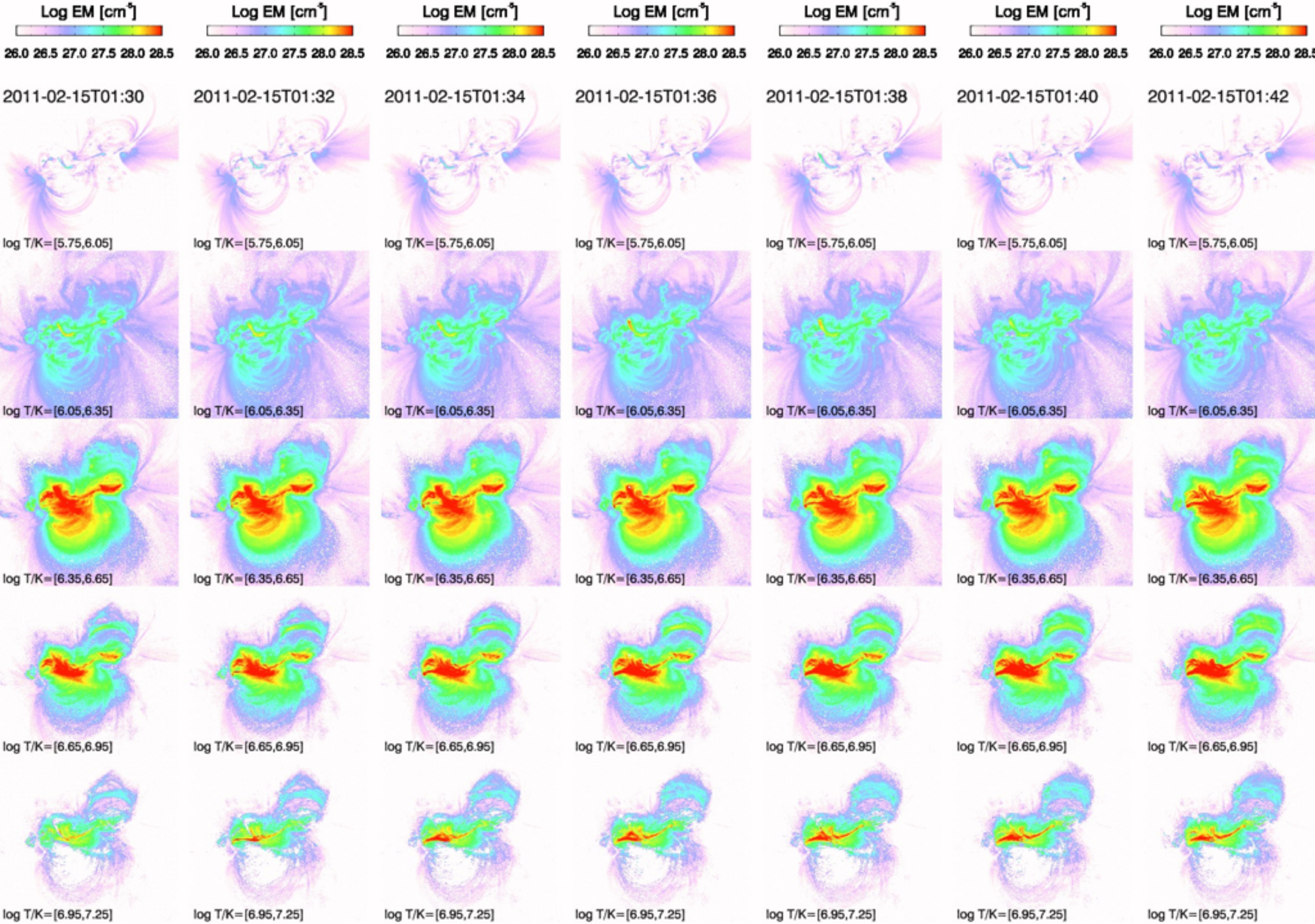
Log EM [cm⁻⁵]
26.0 26.5 27.0 27.5 28.0 28.5
2011-02-15T01:30
2011-02-15T01:32
2011-02-15T01:34
2011-02-15T01:36
2011-02-15T01:38
2011-02-15T01:40
2011-02-15T01:42
log T/K=[5.75,6.05]
log T/K=[6.05,6.35]
log T/K=[6.35,6.65]
log T/K=[6.65,6.95]
log T/K=[6.95,7.25]

Outline

1. Aims
2. What do we see in the EUV channels of AIA?
3. Introduction to the problem of Differential Emission Measure (DEM) Inversions
4. Description of sparse solver for AIA data
5. Tutorial on how to use the AIA_SPARSE_EM package
6. Practice exercises
7. Example science problems to tackle

Active Region Thermal Structure

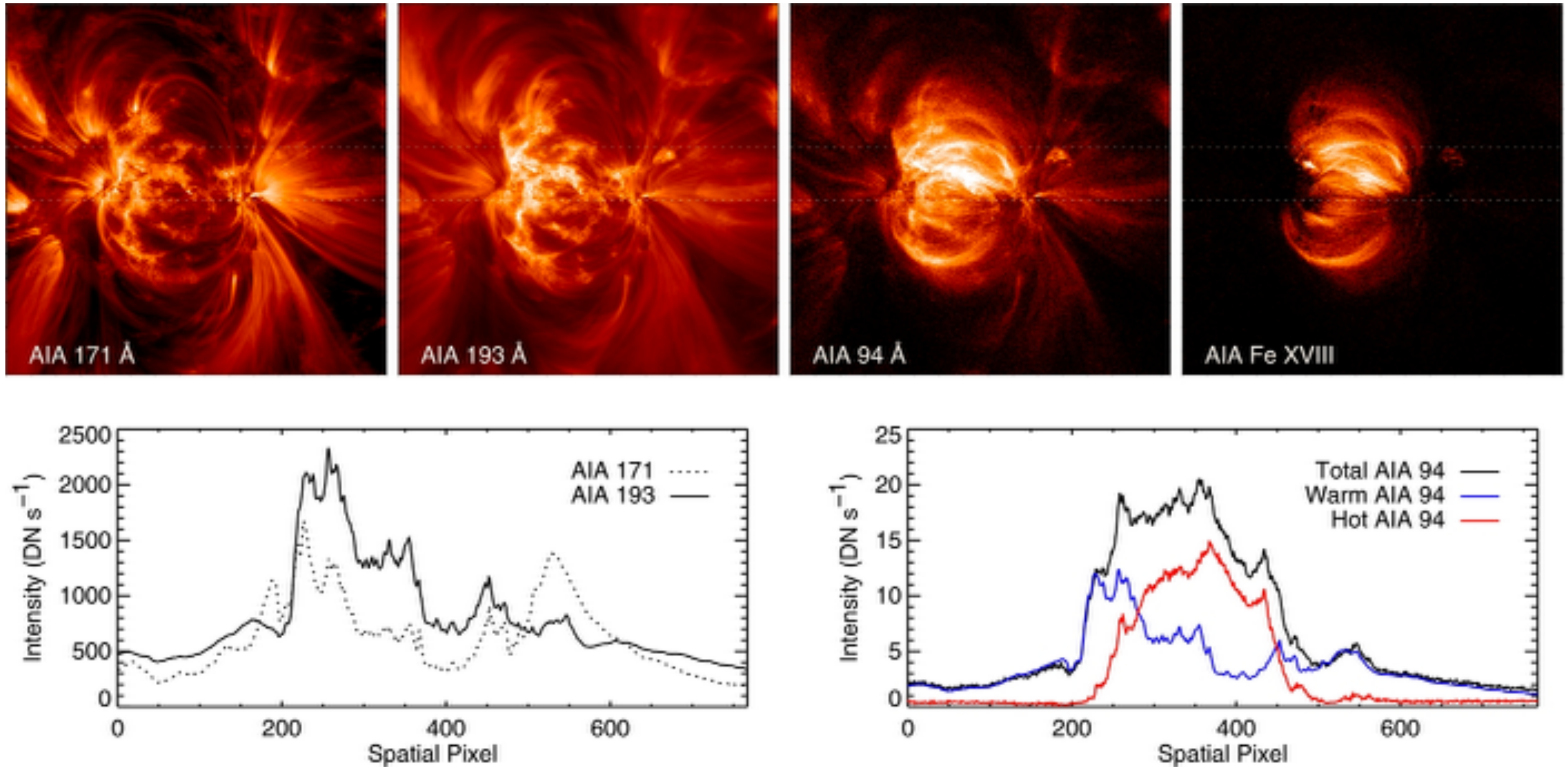

Warren, Winebarger & Brooks (2012) devised a method to separate the ‘warm’ and ‘hot’ components of emission from the AIA 94 Å channel. They use this empirical fit:

$$I_{94\mathrm{warm}} = 0.39 \sum_{i=1}^{4} a_i \left[\frac{f I_{171} + (1-f) I_{193}}{116.54} \right]^i$$

“for this value of f [=0.3], the coefficients to the polynomial fit are -7.31×10^{-2}, 9.75×10^{-1}, 9.90×10^{-2}, and -2.84×10^{-3}.”

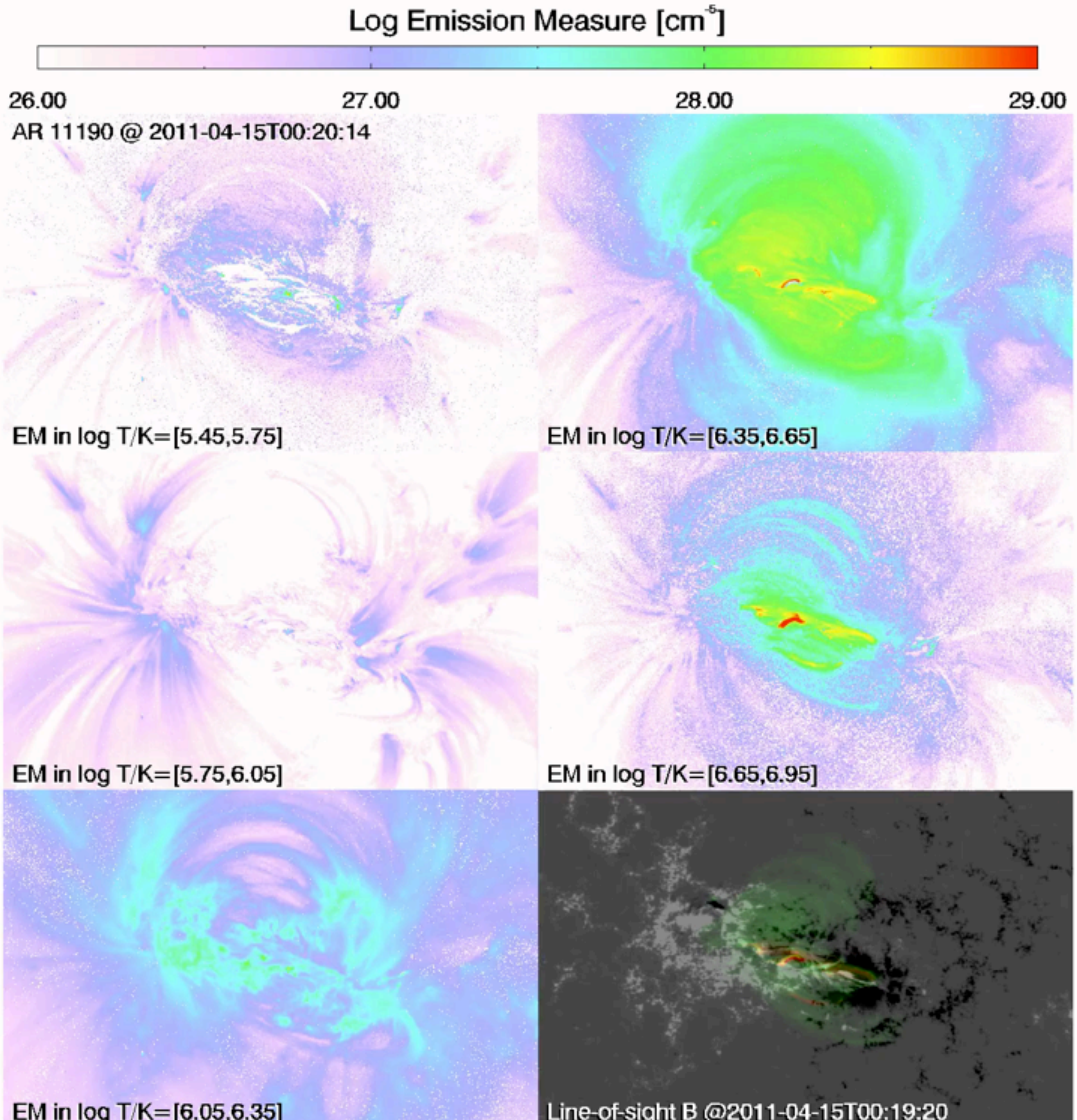

Log Emission Measure [cm^{-5}]
26.00
27.00
28.00
29.00
AR 11190 @ 2011-04-15T00:20:14
EM in log T/K=[5.45,5.75]
EM in log T/K=[6.35,6.65]
EM in log T/K=[5.75,6.05]
EM in log T/K=[6.65,6.95]
EM in log T/K=[6.05,6.35]
Line-of-sight B @2011-04-15T00:19:20

Workshop Practice Exercise 1:

AR 11190

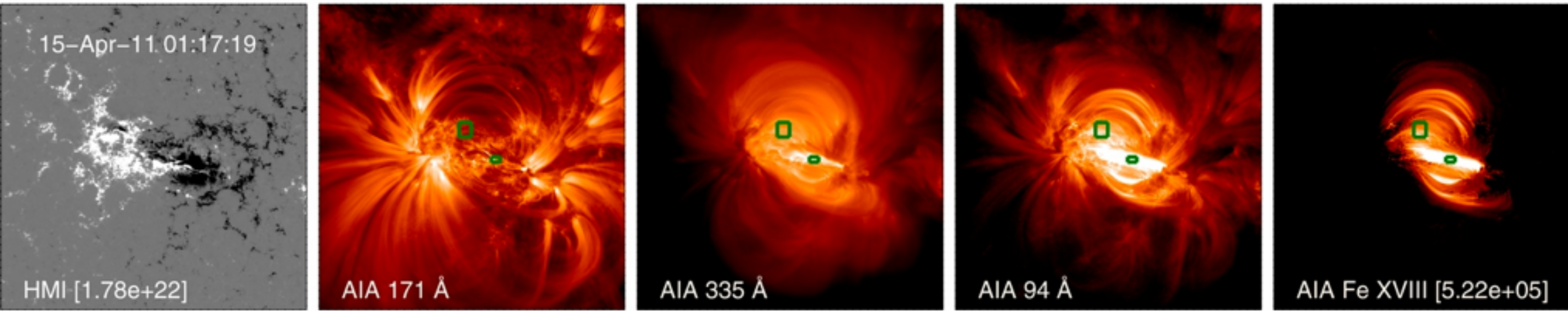

From: Warren, Winebarger & Brooks (2012)

<u>Go to http://www.lmsal.com/~cheung/AIA/ar11190/</u>
Download a genx file and plot the DEM distribution in regions marked by the green boxes.

How do the DEMs in these boxes evolve?
What about the DEM averaged over the AR? (Take care with pixels that have no DEM solutions).

Workshop Practice Exercise 2:

AR 11190

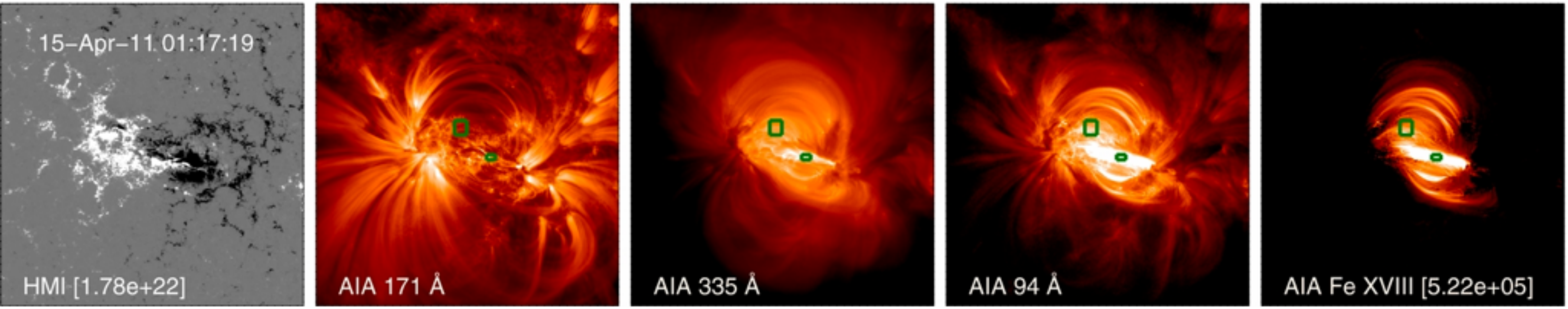

From: Warren, Winebarger & Brooks (2012)

Go to http://www.lmsal.com/~cheung/AIA/11190/
Download a genx file
Starting from the DEM solution, generate AIA 94 images separately for the 'warm' and 'hot' components.

Hint: use
PRO AIA_SPARSE_EM_EM2IMAGE, em, image=image, status=status

Workshop Practice Exercise 3:
Examine impact of choice of basis functions

- By default, aia_sparse_em_init uses 4 sets of basis functions (Dirac + 3 sets of truncated gaussians).
- Default keyword is bases_sigmas = [0,0.1,0.2,0.6]
- Test how choosing other basis sets changes DEM results. e.g.
  - Only Dirac Delta functions bases_sigmas = [0]
  - Dirac + Gaussians of width 0.1 bases_sigmas = [0,0.1]
  - Dirac + Gaussians of width 0.1, 0.2 and 0.3 bases_sigmas = [0,0.1,0.2,0.3]

Workshop Practice Exercise 4: AIA + XRT DEM inversions

- Joint AIA-XRT DEM inversions
- Download aiaxrt.pro from http://tinyurl.com/aiadem
    - .compile aia_sparse_em_init
    - .r aiaxrt
- This script solves uses sample AIA data to solve for a DEM cube. Then it synthesizes AIA and XRT images. Then it uses AIA+XRT for DEM inversion.

Outline

1. Aims

2. What do we see in the EUV channels of AIA?

3. Introduction to the problem of Differential Emission Measure (DEM) Inversions

4. Description of sparse solver for AIA data

5. Tutorial on how to use the AIA_SPARSE_EM package

6. Practice exercises

7. **Example science problems to tackle: 13:15pm today**

Science Cases

- Thermal evolution of active regions from emergence to decay
- Thermodynamic structure of reconnection outflows
- From chromospheric evaporation to catastrophic condensation

Science Case 1) Emerging Flux

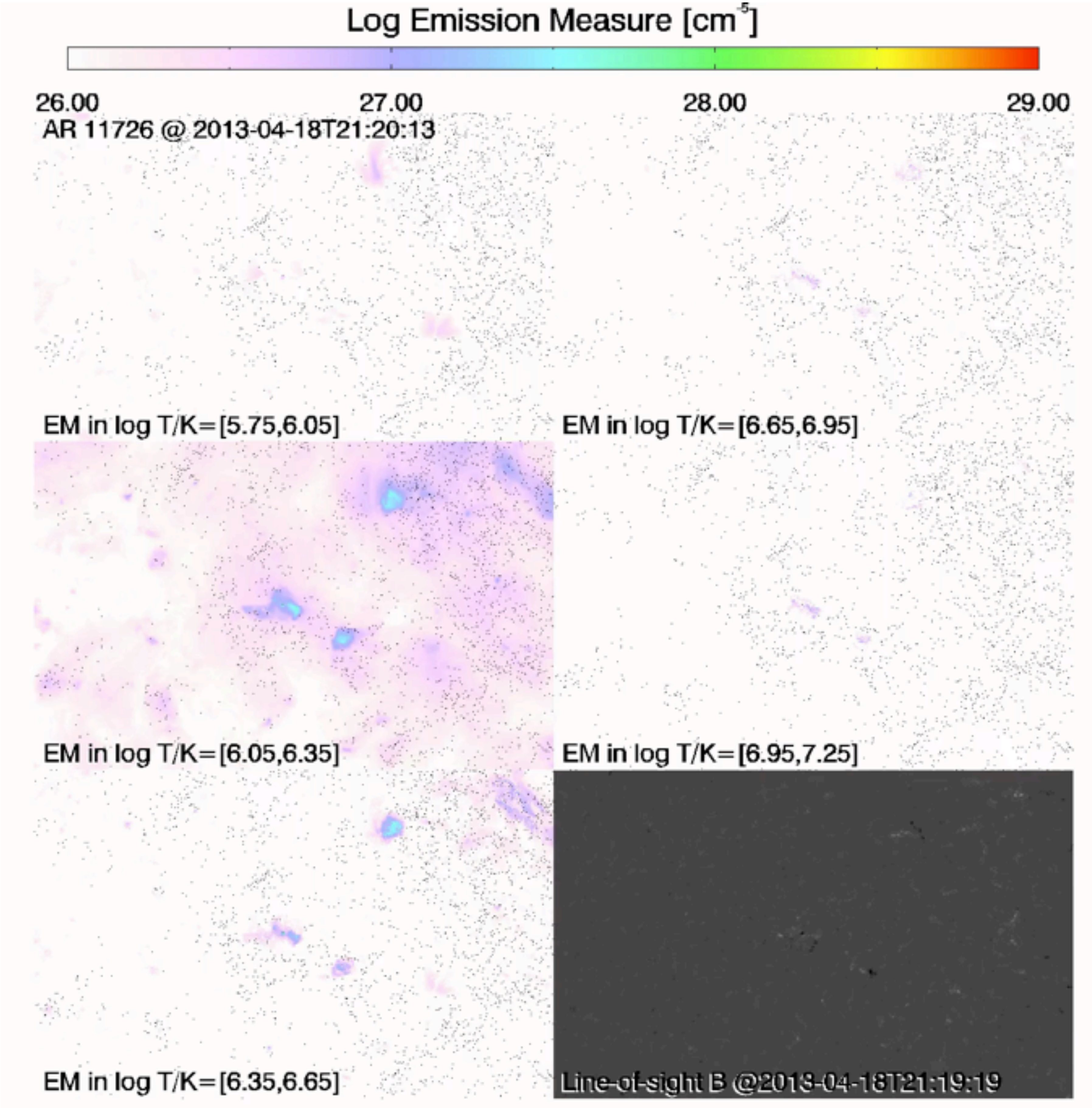

<u>DEM movie of the emergence of AR 11726</u>

<u>Other panels:</u>
EM in various log T bins

<u>Lower right panel only</u>
Greyscale:
B_{los} from HMI
Green: 6MK EM
Yellow/Red: 10 MK EM

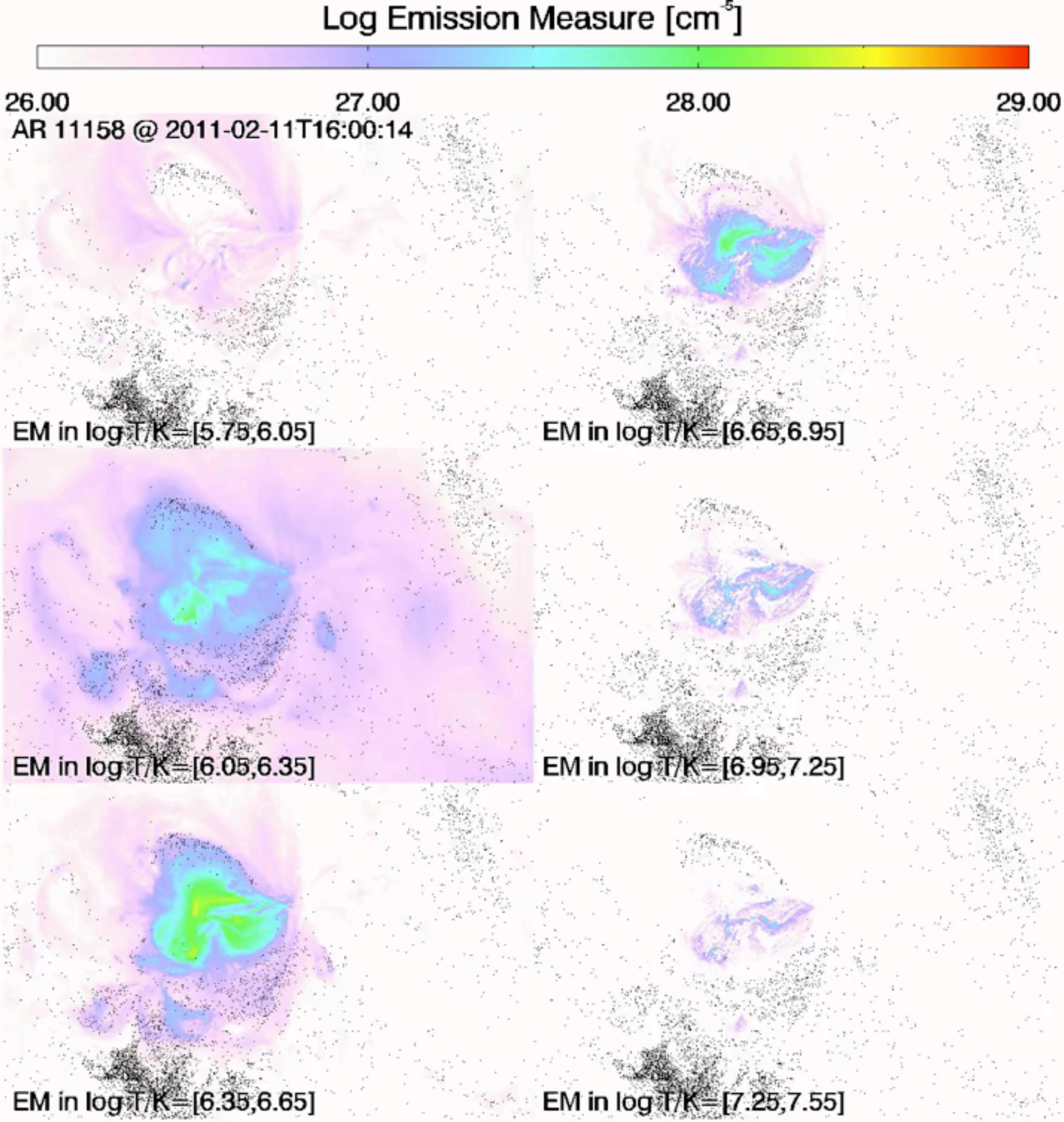

DEM movie of the emergence of AR 11158

Black pixels are where no solutions were found

Science Case 2) Reconnection Outflows

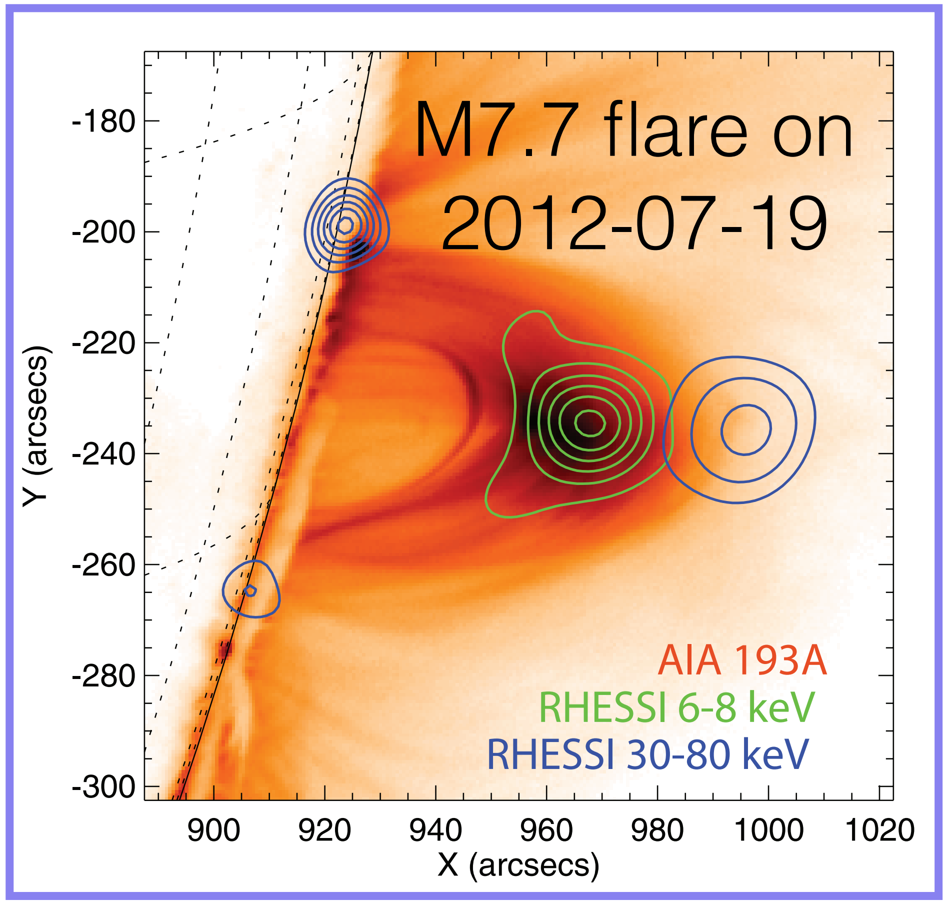

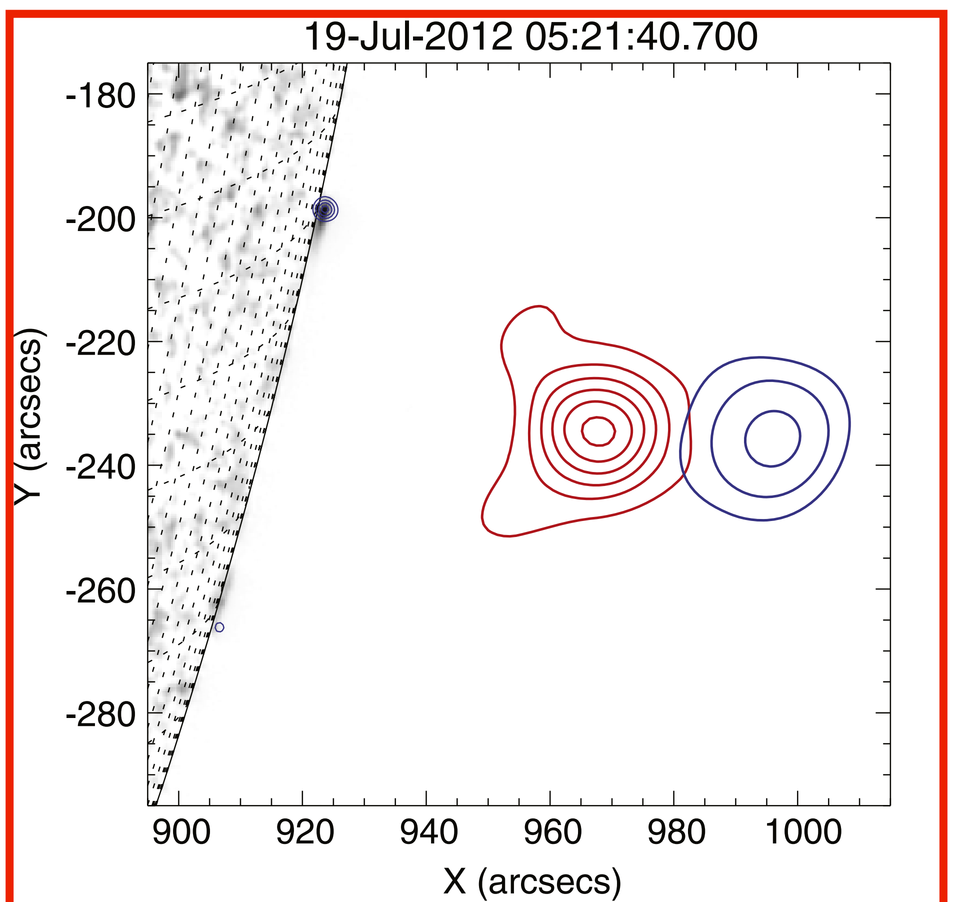

Selected scientific studies of this flare:

- Patsourakos, Vourlidas & Stenborg, 2013, ApJ, **764**, 125: **Prior confined eruption produced a pre-existing coronal flux rope, which then erupted to give the M7.7 flare.**
- Wei Liu, Chen & Petrosian, 2013, ApJ, **767**, 168: **Detailed timeline of sequence of events including timing and propagation of EUV and X-ray sources.**
- Rui Liu, 2013, MNRAS, **434**, 1309: **Same onset time for HXR and microwave (Nobeyama RH data) bursts.**
- Krücker & Battaglia , 2014, ApJ, **780**, 107: **Ratio of thermal protons (from AIA) to non-thermal electrons (from RHESSI HXR) in loop-top source is of order 1.**
- Sun, Cheng & Ding, 2014, ApJ, **786**, 73: **Performed a very detailed DEM (imaging) analysis of this flare. They used xrt_iterative_dem2.pro (code by M. Weber, non-linear least square inversion with splines).**
- Krücker et al., 2015, ApJ, **802**, 19: **HMI white light (WL) enhancement at footprint co-incident with HXR footpoint source. Interpretation: energy deposition by non-thermal electrons is radiated away and does not cause chromospheric evaporation.**

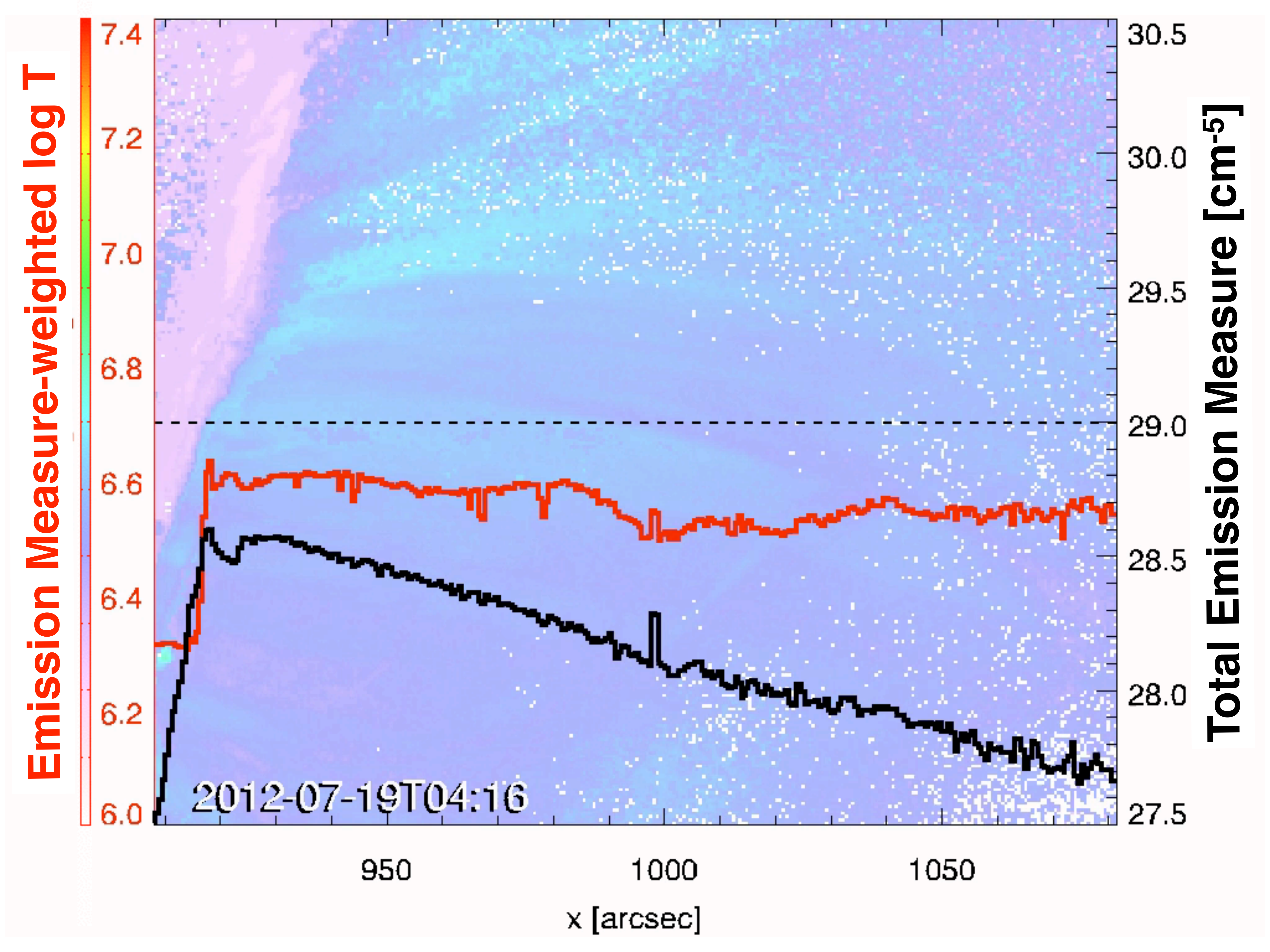
Emission Measure-weighted log T
7.4
7.2
7.0
6.8
6.6
6.4
6.2
6.0
Total Emission Measure [cm^{-5}]
30.5
30.0
29.5
29.0
28.5
28.0
27.5
2012-07-19T04:16
950
1000
1050
x [arcsec]

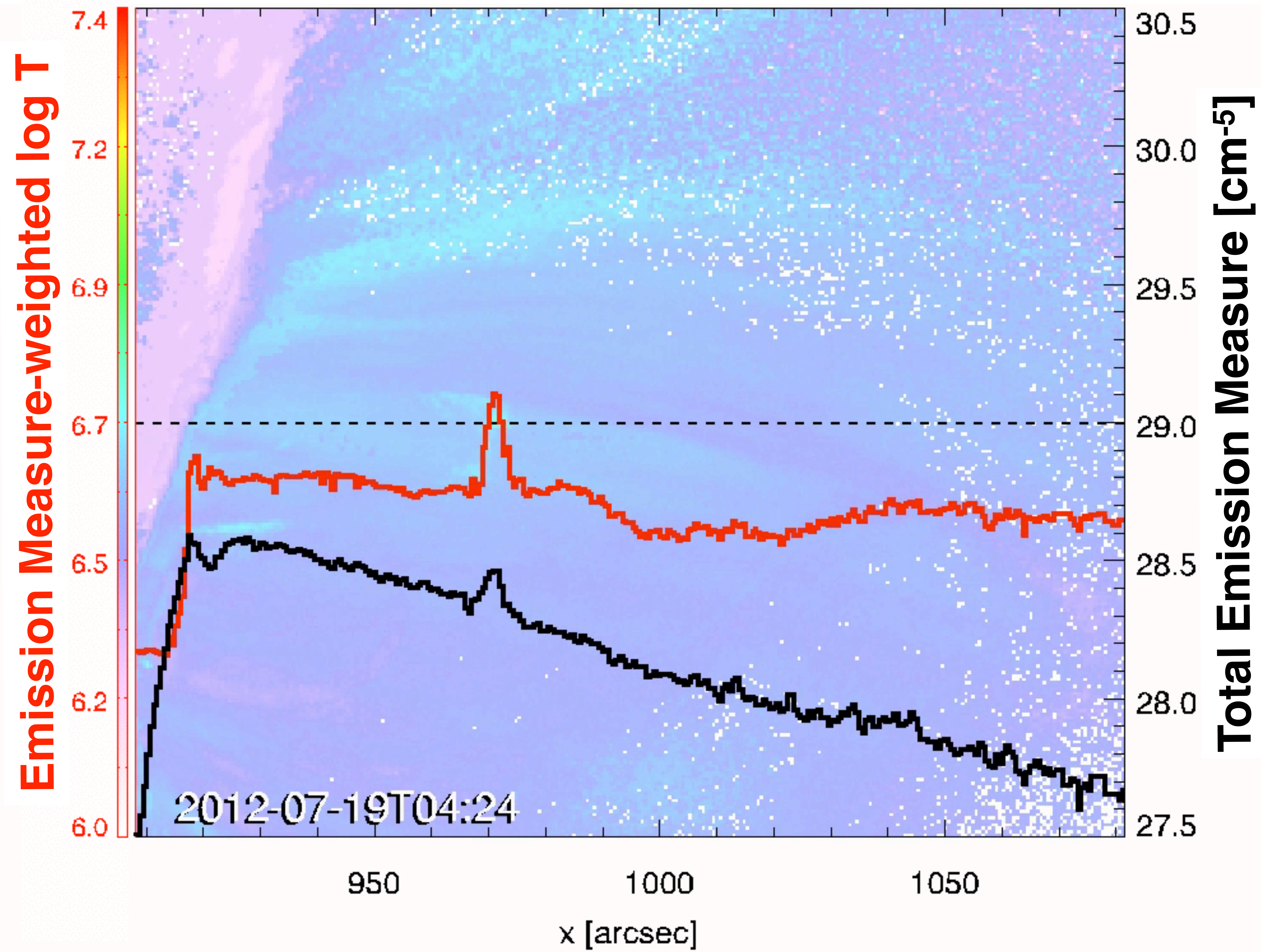

Emission Measure-weighted log T
Total Emission Measure [cm-5]
x [arcsec]
2012-07-19T04:24
7.4
7.2
6.9
6.7
6.5
6.2
6.0
30.5
30.0
29.5
29.0
28.5
28.0
27.5
950
1000
1050

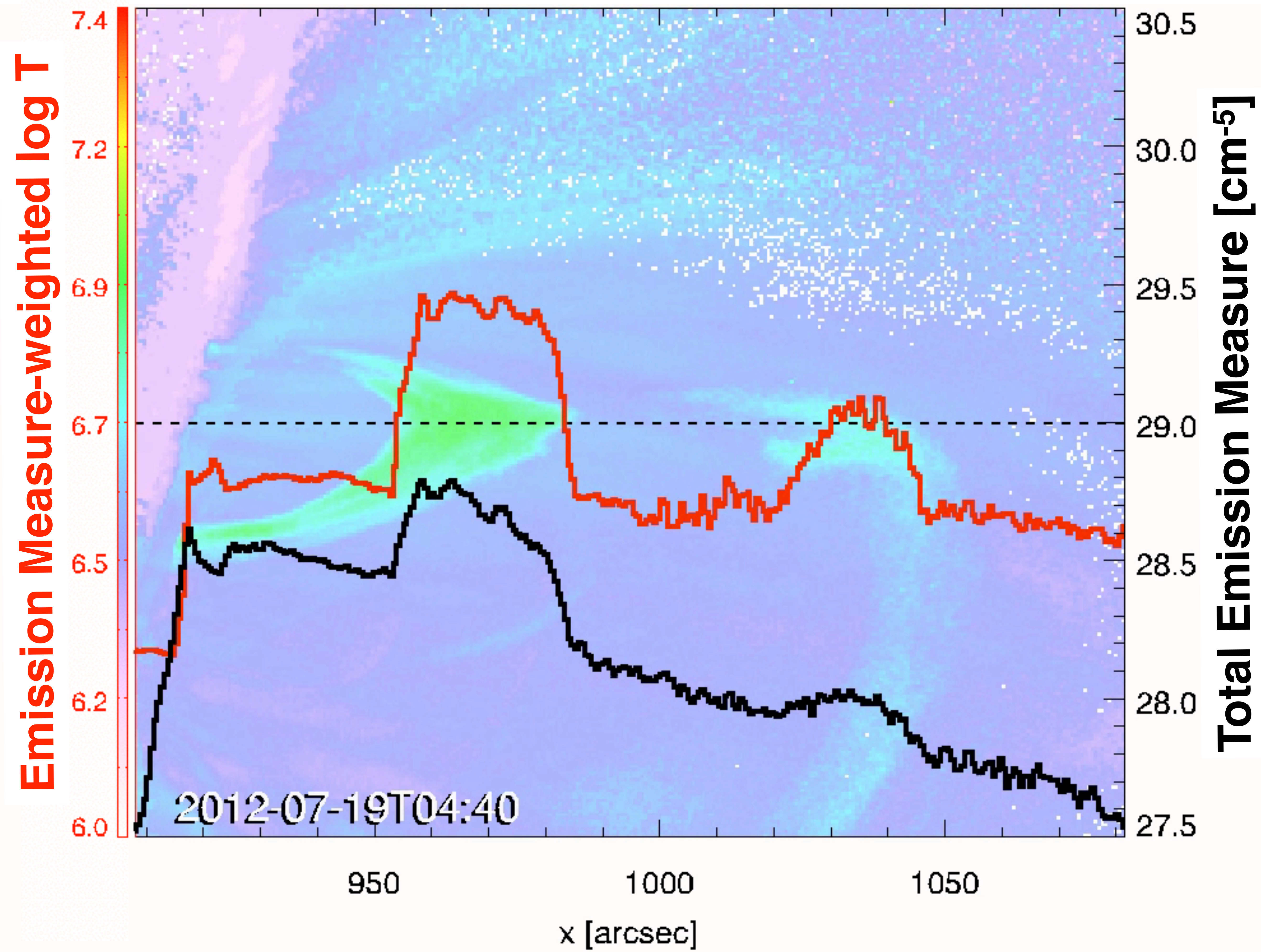

Emission Measure-weighted log T
7.4
7.2
6.9
6.7
6.5
6.2
6.0
Total Emission Measure [cm-5]
30.5
30.0
29.5
29.0
28.5
28.0
27.5
2012-07-19T04:40
950
1000
1050
x [arcsec]

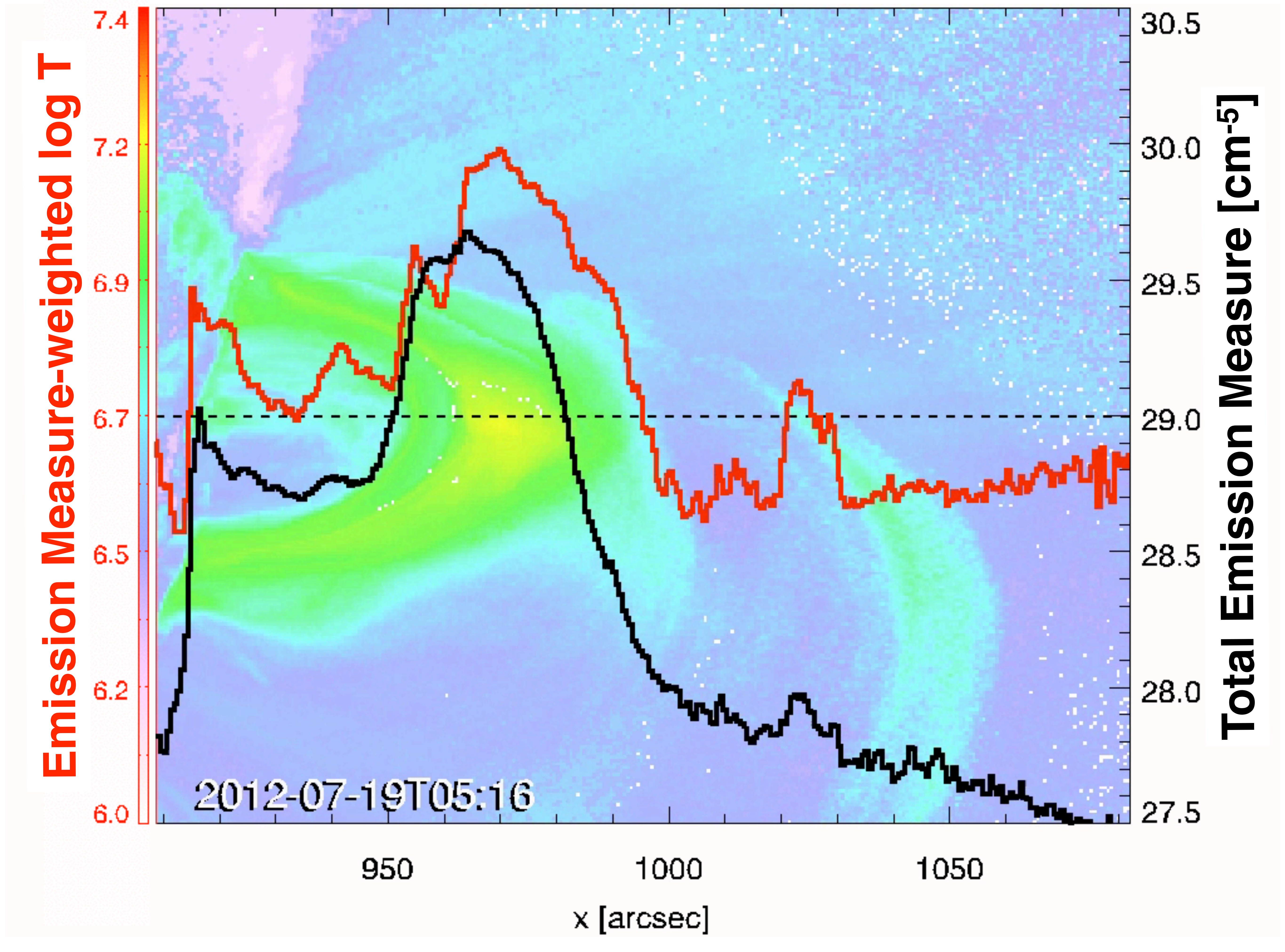

Emission Measure-weighted log T
7.4
7.2
6.9
6.7
6.5
6.2
6.0
30.5
30.0
29.5
29.0
28.5
28.0
27.5
Total Emission Measure [cm^{-5}]
2012-07-19T05:16
950
1000
1050
x [arcsec]

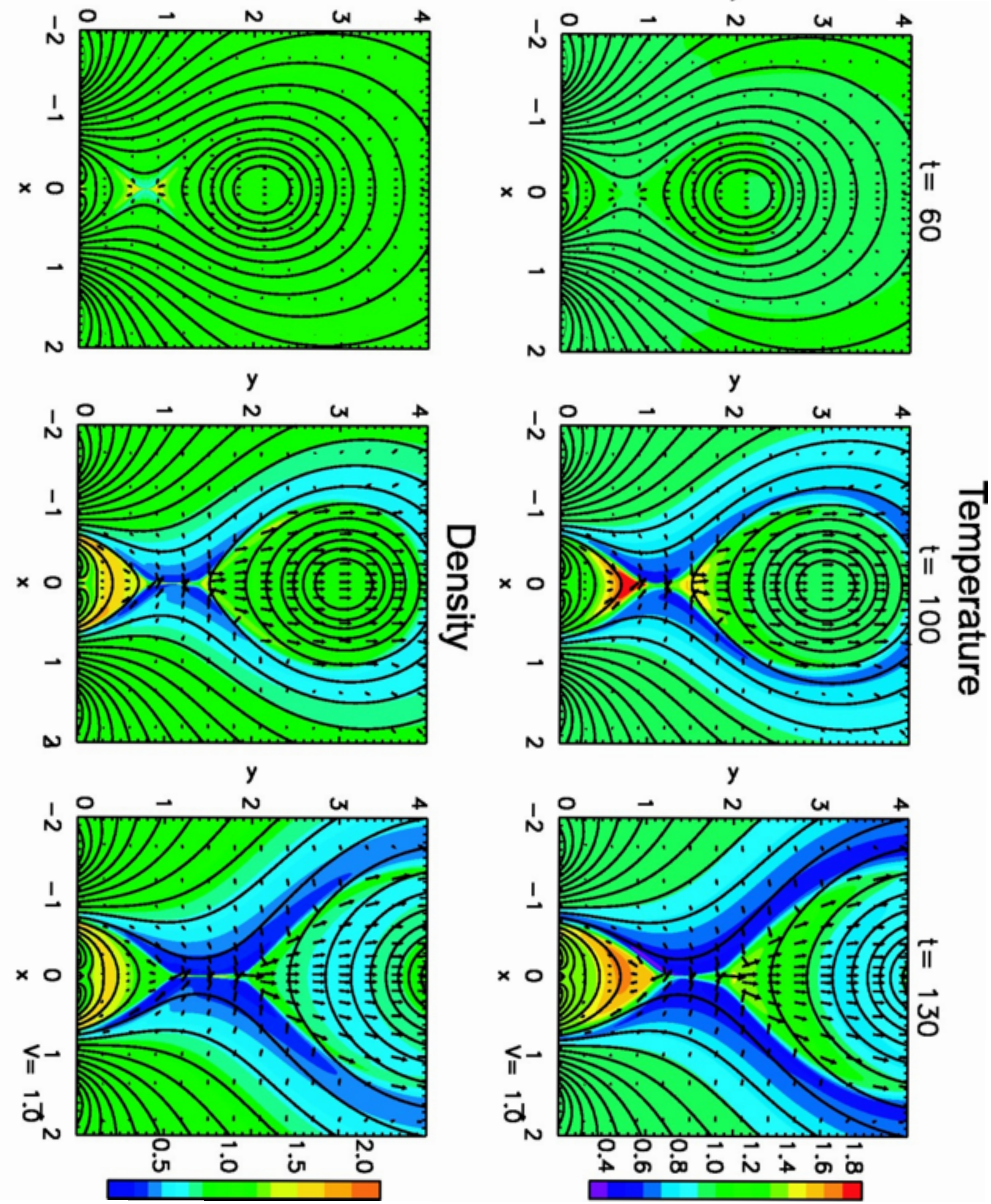

Shiota et al. (2005, ApJ, **634**, 663):

- 2.5D MHD simulation of of the eruption of a pre-existing flux rope triggered by flux emergence.
- Similar scenario as modeled by Chen & Shibata (2000, ApJ, **545**, 524) but with field-aligned thermal conduction.
- Both temperature and density are initially uniform (dimensionless value of unity).

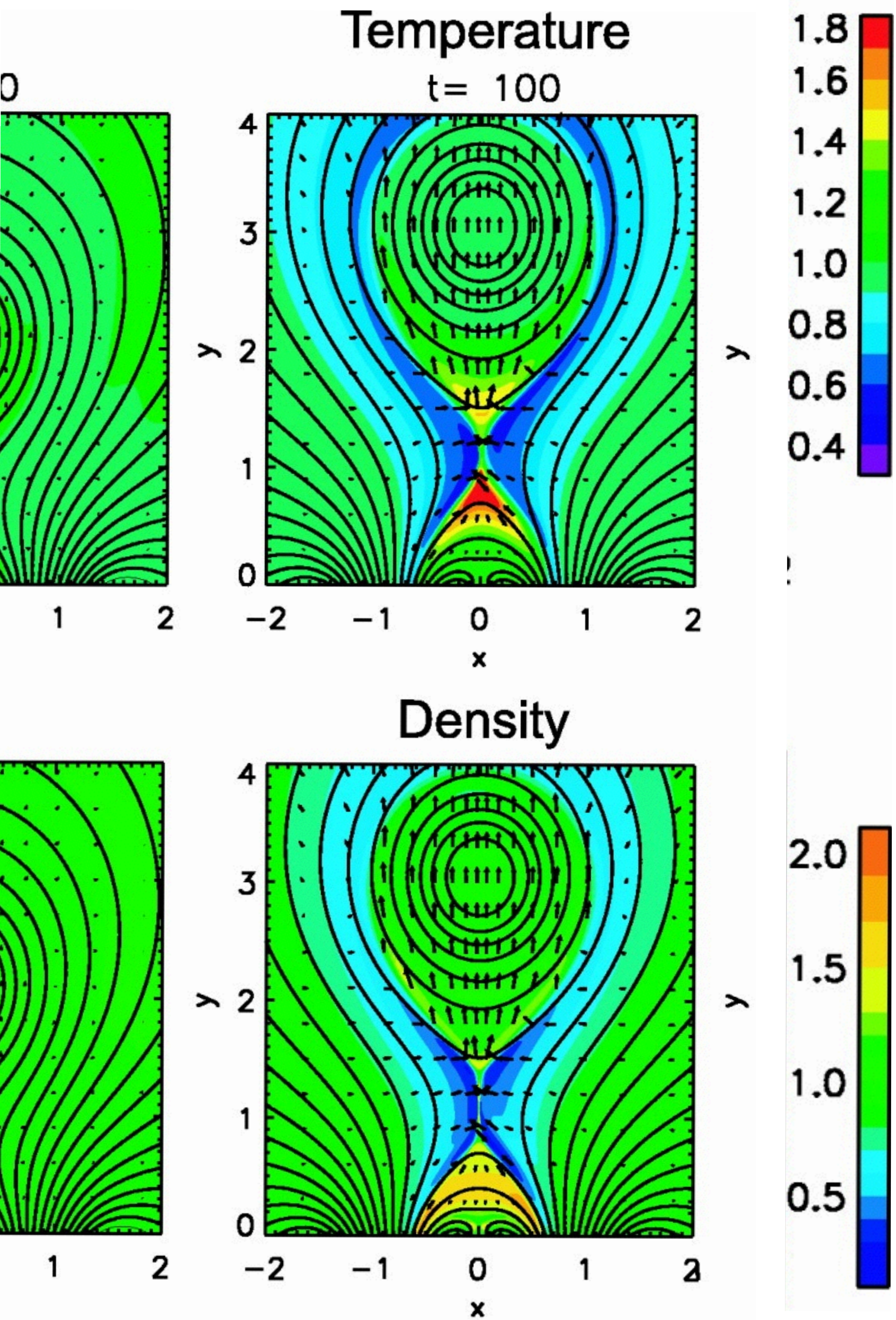

Temperature
t= 100
Density
x
y

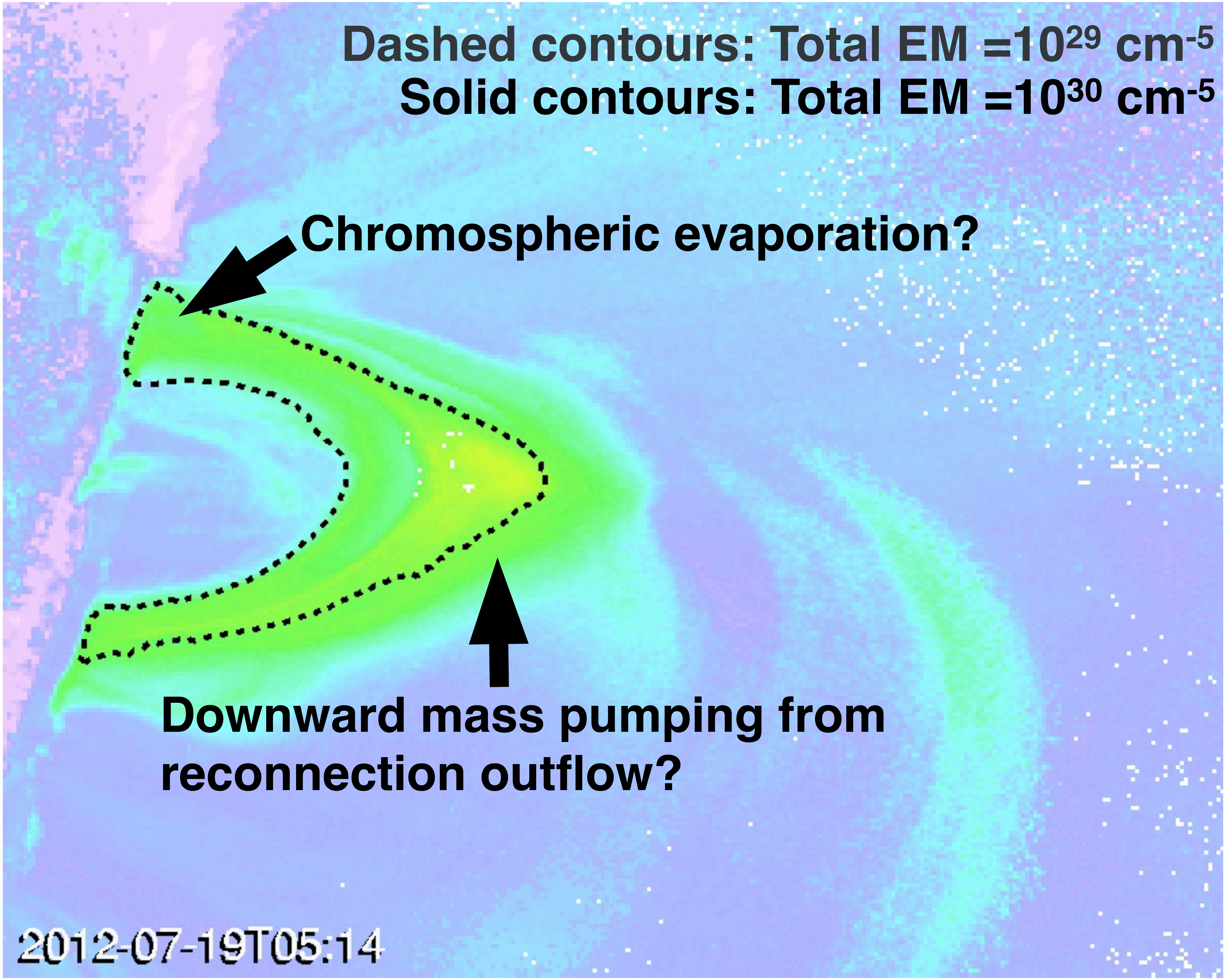
Dashed contours: Total EM =10^{29} cm^{-5}
Solid contours: Total EM =10^{30} cm^{-5}
Chromospheric evaporation?
Downward mass pumping from reconnection outflow?
2012-07-19T05:14

Influence of efficiency of thermal conduction / system size

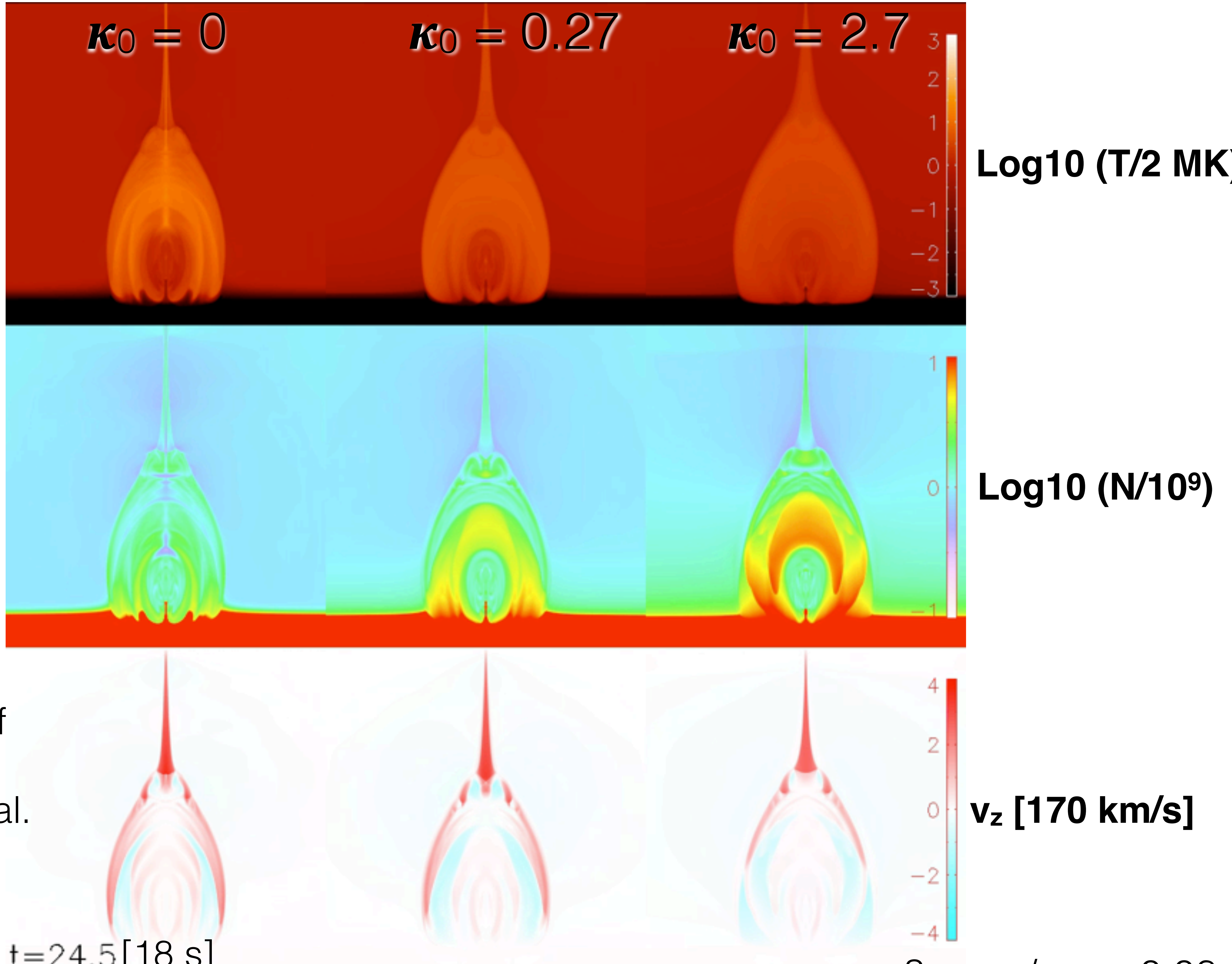

Extension of study by Takasao et al. (ApJ, 2015, **805**, 135)

$\beta = p_g / p_m = 0.08$

Influence of efficiency of thermal conduction / system size

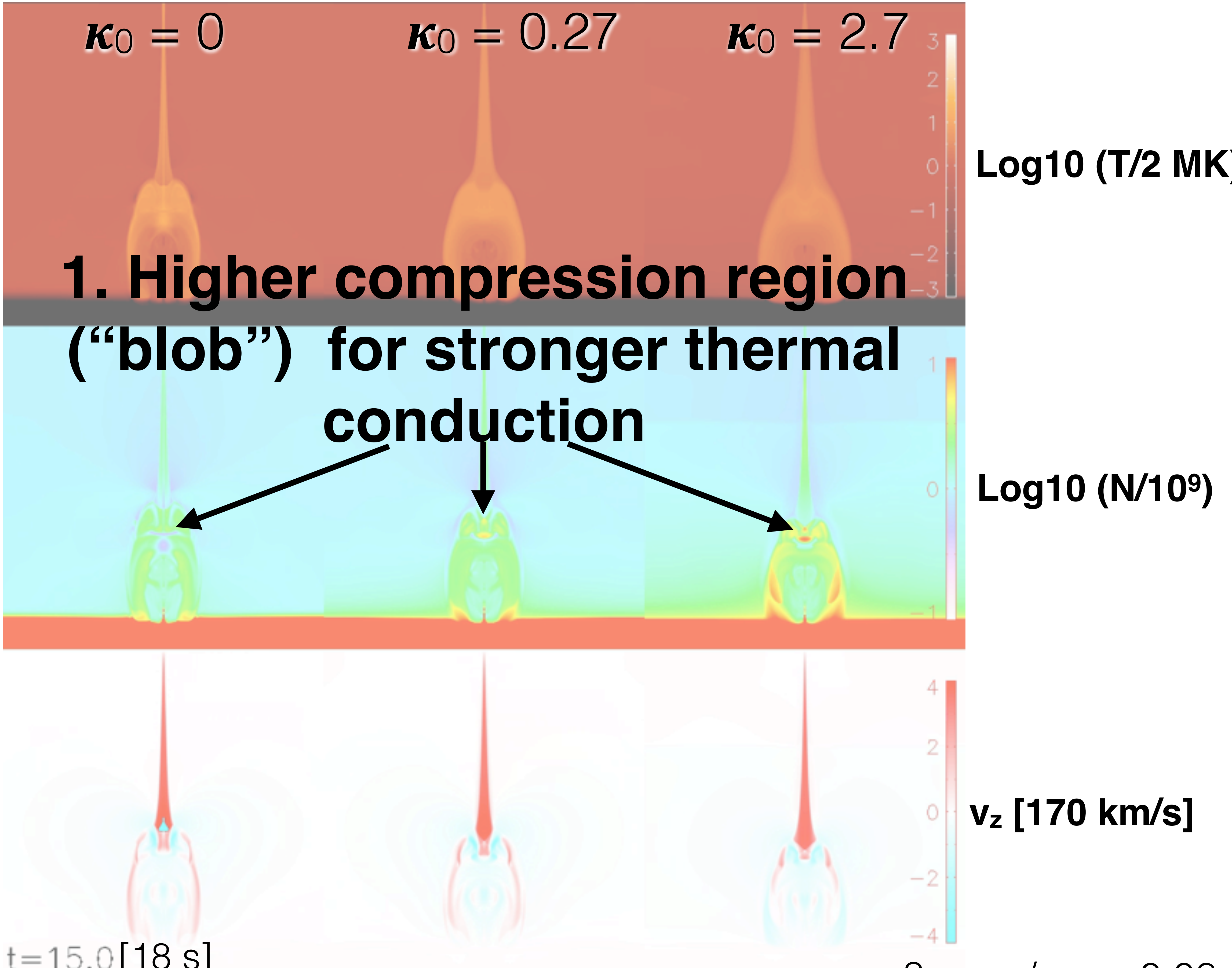

$\beta = p_g / p_m = 0.08$

Influence of efficiency of thermal conduction / system size

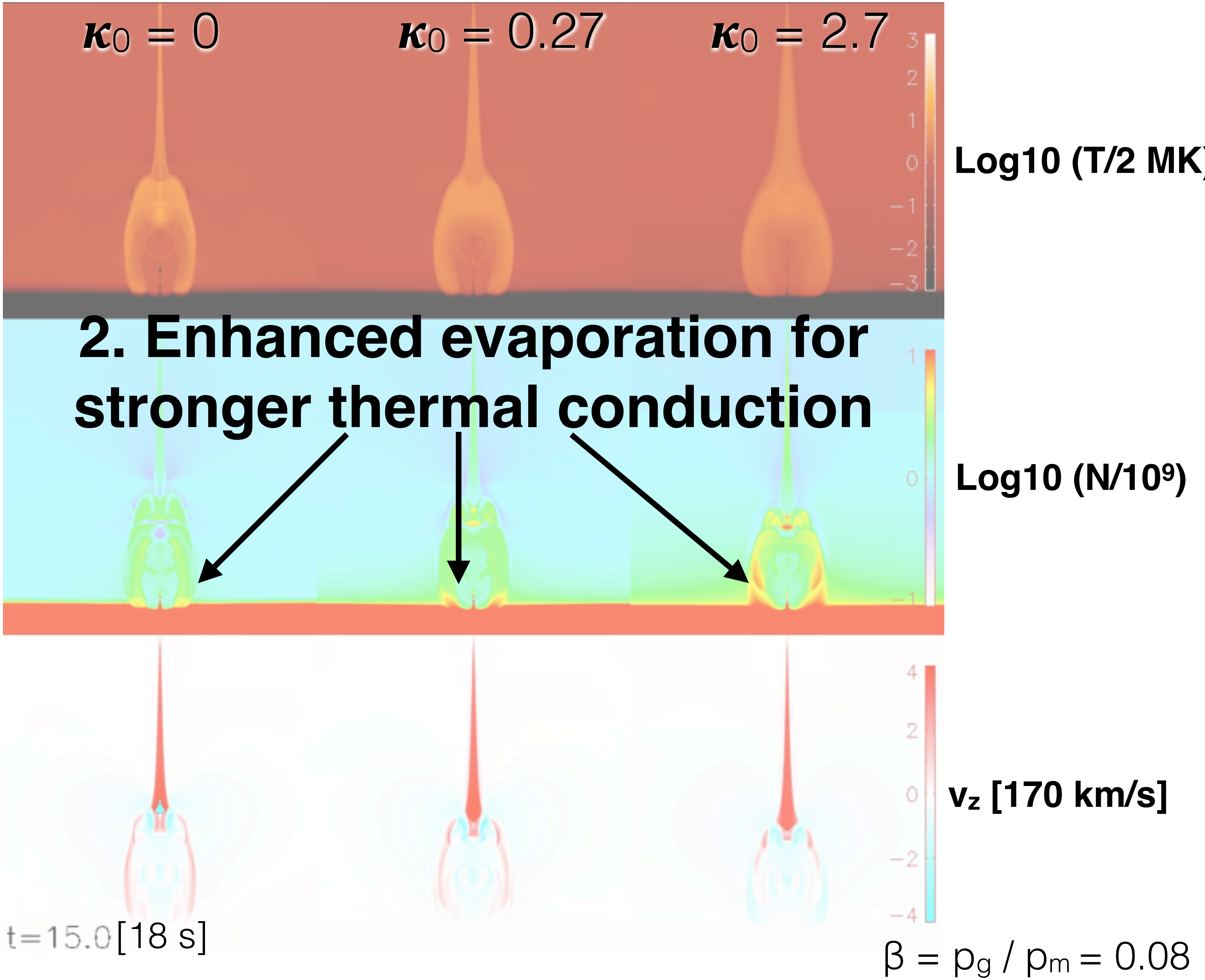

Long Duration
GOES C6.7 flare

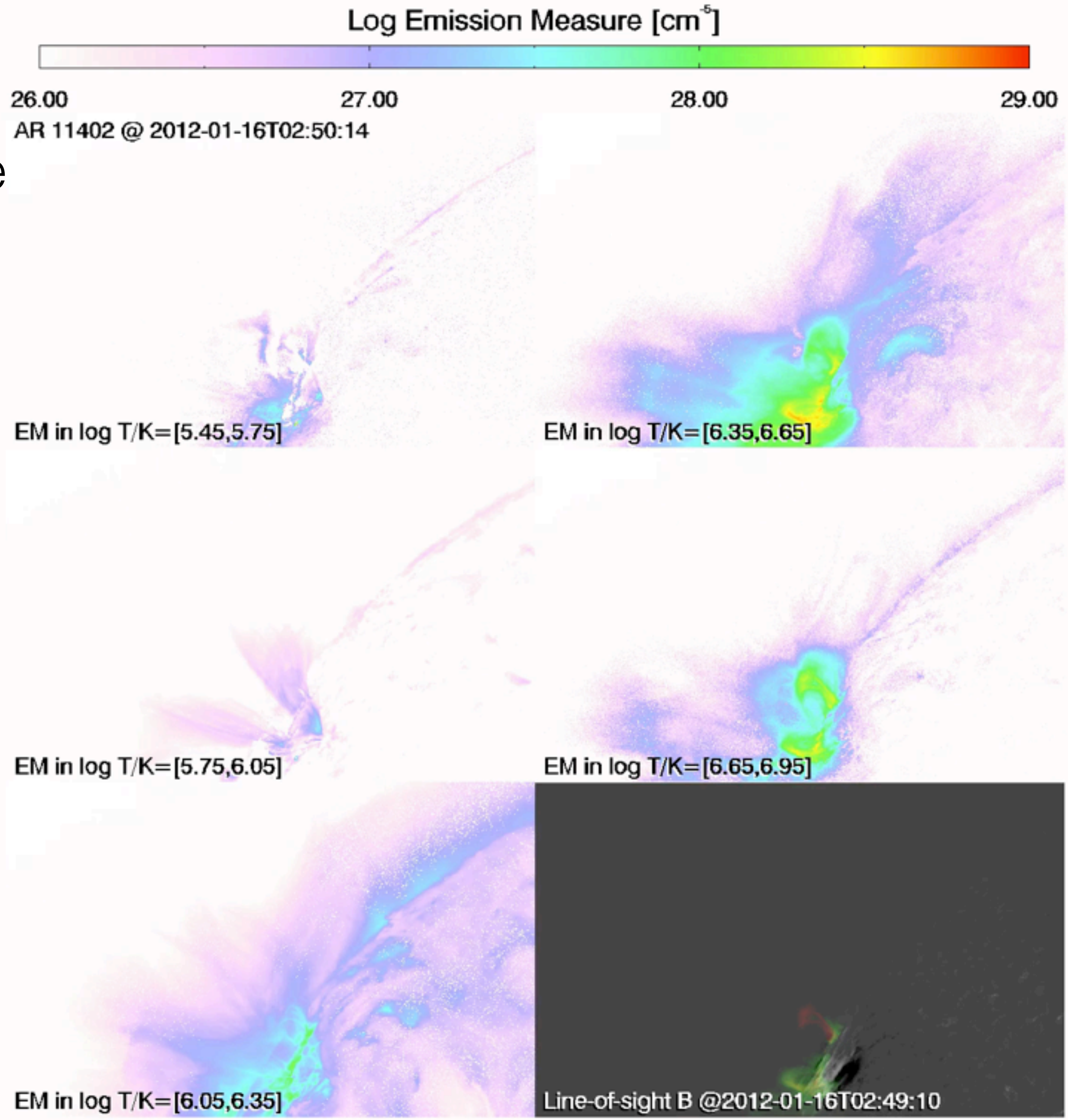

Some remarks

- AIA differential emission measure inversions (e.g. using the method of Cheung et al. 2015; http://tinyurl.com/aiadem) can be used to quantitatively study the thermal evolution of flare plasma.
- The efficiency of thermal conduction / system size impacts:
    1. The density enhancement in deceleration region of the reconnection outflow, and
    2. The amount of evaporated material.
- Observations can possibly help us test whether classical Spitzer thermal conduction is appropriate or should be modified (e.g. Imada, Murakami & Watanabe, PoP, 2015, **22**, 10; Wang et al., 2015, ApJL, **811**, L13).
- Future work:
    - Should measure 1. and 2. in a systematic study of flares to test sensitivity to system size / efficiency of thermal conduction.
    - Use 3D MHD simulations of flares for forward modeling of observables.

Science Case 3) Chromospheric Evaporation & Condensation

Observations

Spectra covering temperatures from 4,500 K to 10 MK

Images covering temperatures from 4,500 K to 65,000 K

Baseline: 5s for slit-jaw images, 1s for 6 spectral windows, rapid rastering

Predicted Count Rates

Ion Spectrum	λ	Δλ	Log T	Estimated Count Rate (counts/s/line/spatial pixel)			Detector
	Å	mÅ	K	Quiet Sun	Active Region	Flare	
UV Spectra (effective area of 2.8 cm^2 for far-UV, 0.3 cm^2 for Mg passband, continuum is 1 Å) †: Count rates for Mg II wing, h and k are in counts/s/spectral pixel/spatial pixel							
Si I (3P) Cont	1335	12.5	3.7	40	80	---	1
Mg II wing	2820	25	3.7-3.9	2100†	7500†	7500†	3
O I	1356	12.5	3.8	50	100	250	1
Mg II h	2803	25	4.0	870†	3400†	13000†	3
Mg II k	2796	25	4.0	1100†	4500†	10000†	3
C II	1335	12.5	4.3	540	1970	22000	1
C II	1336	12.5	4.3	500	1780	20000	1
Si IV	1403	12.5	4.8	400	1000	1e6	2
Si IV	1394	12.5	4.8	640	2200	3e6	2
O IV	1401	12.5	5.2	65	116	2e5	2
O IV	1400	12.5	5.2	25	60	1e5	2
Fe XII	1349	12.5	6.2	30	50	500	1
Fe XXI	1354	12.5	7.0	10	40	4e4	1
UV Slit-Jaw Images				**Estimated Count Rate (counts/s/pixel)**			
Effective area 0.005 cm^2 with 4 Å FWHM filter for Mg II; 0.7 cm^2 with 40 Å FWHM for far-UV.							
Mg II wing	2831		3.7-3.9	2300	5300	5300	4
Mg II k	2796		4.0	750	3500	8500	4
C II	1335		4.3	400	1300	13000	4
Si IV	1400		4.8	300	1200	2e5	4

From the IRIS poster @ iris.lmsal.com

IRIS is designed to probe the chromosphere and transition region, but it also sees flare plasma (Fe XXI @10 MK).

What about the temperature range in between?

Joint observations between IRIS andAIA to fill the temperature gap.

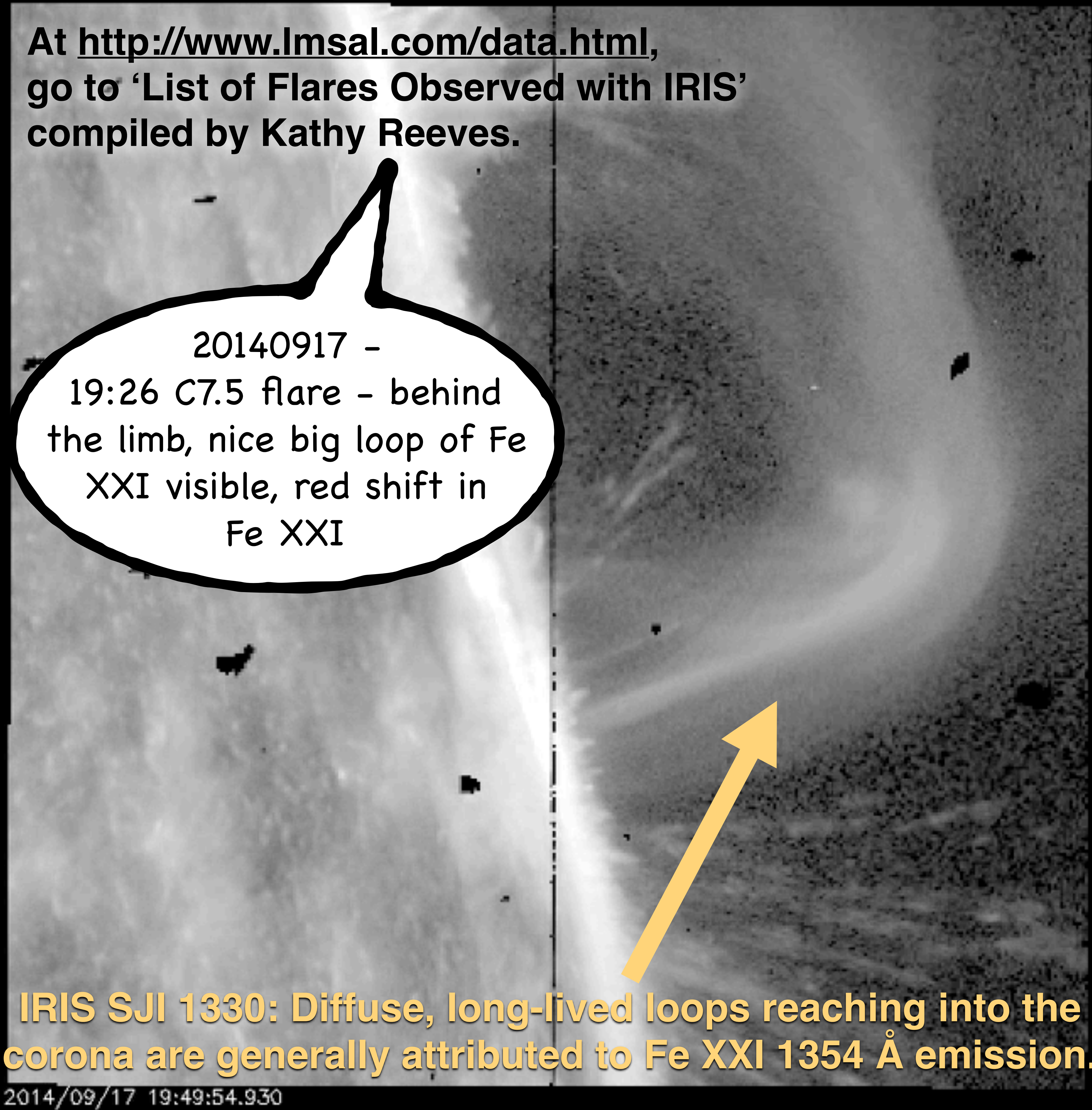
At http://www.lmsal.com/data.html,
go to ‘List of Flares Observed with IRIS’
compiled by Kathy Reeves.
20140917 - 19:26 C7.5 flare - behind the limb, nice big loop of Fe XXI visible, red shift in Fe XXI
IRIS SJI 1330: Diffuse, long-lived loops reaching into the corona are generally attributed to Fe XXI 1354 Å emission.
2014/09/17 19:49:54.930

IRIS SJI 1330: Likely Fe XXI 1354 Å emission.

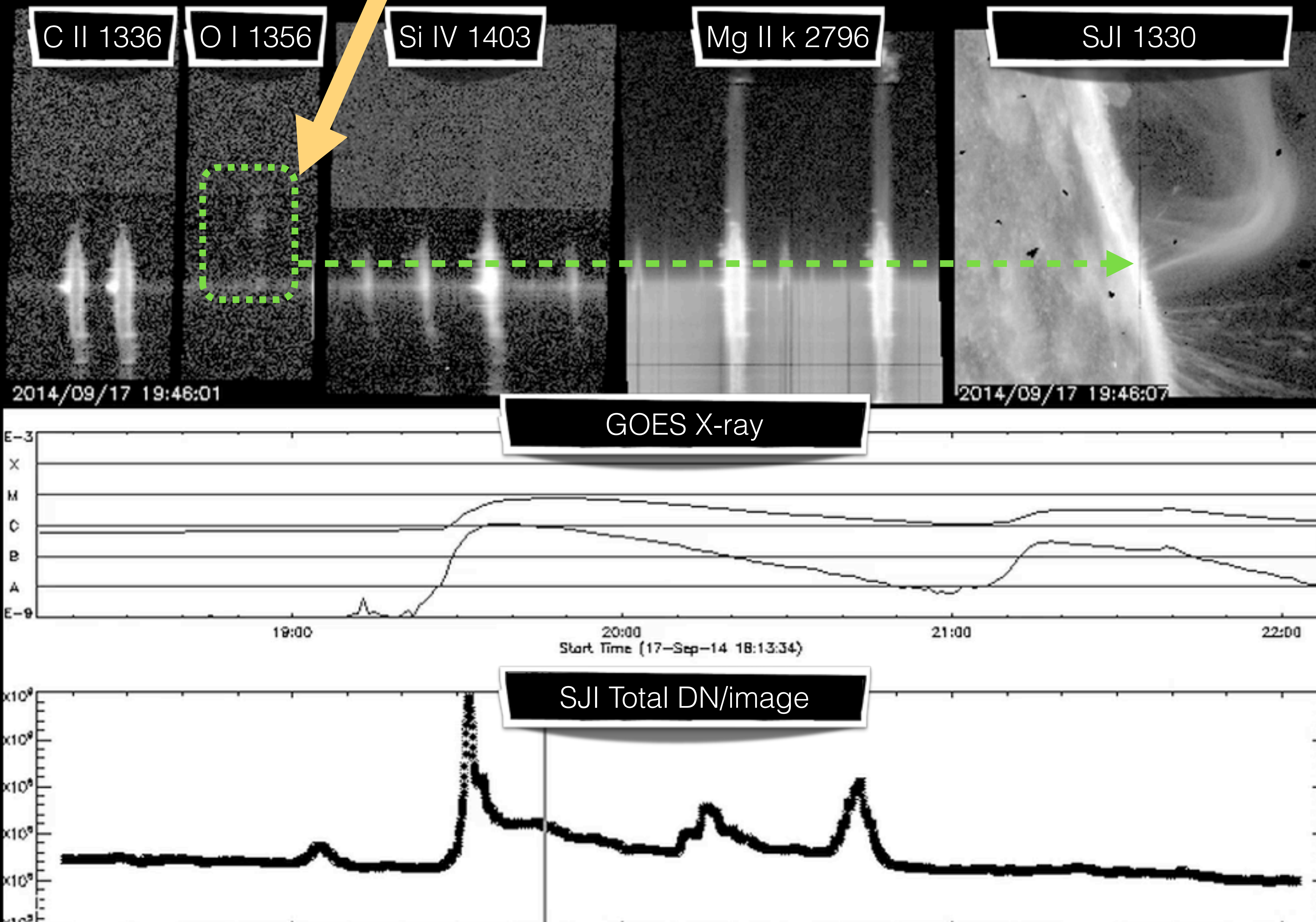

IRIS SJI 1330: Likely Fe XXI 1354 Å emission.

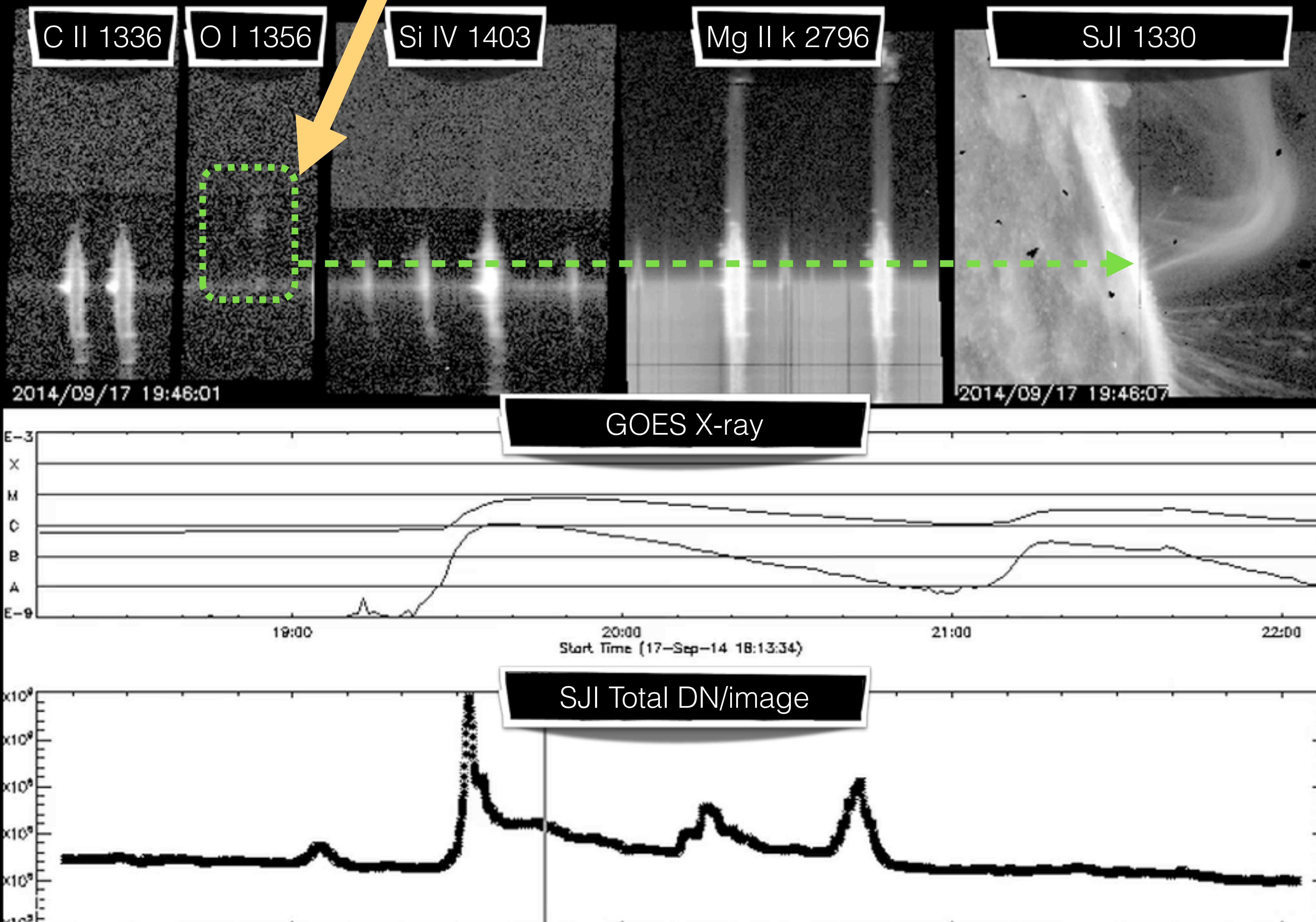

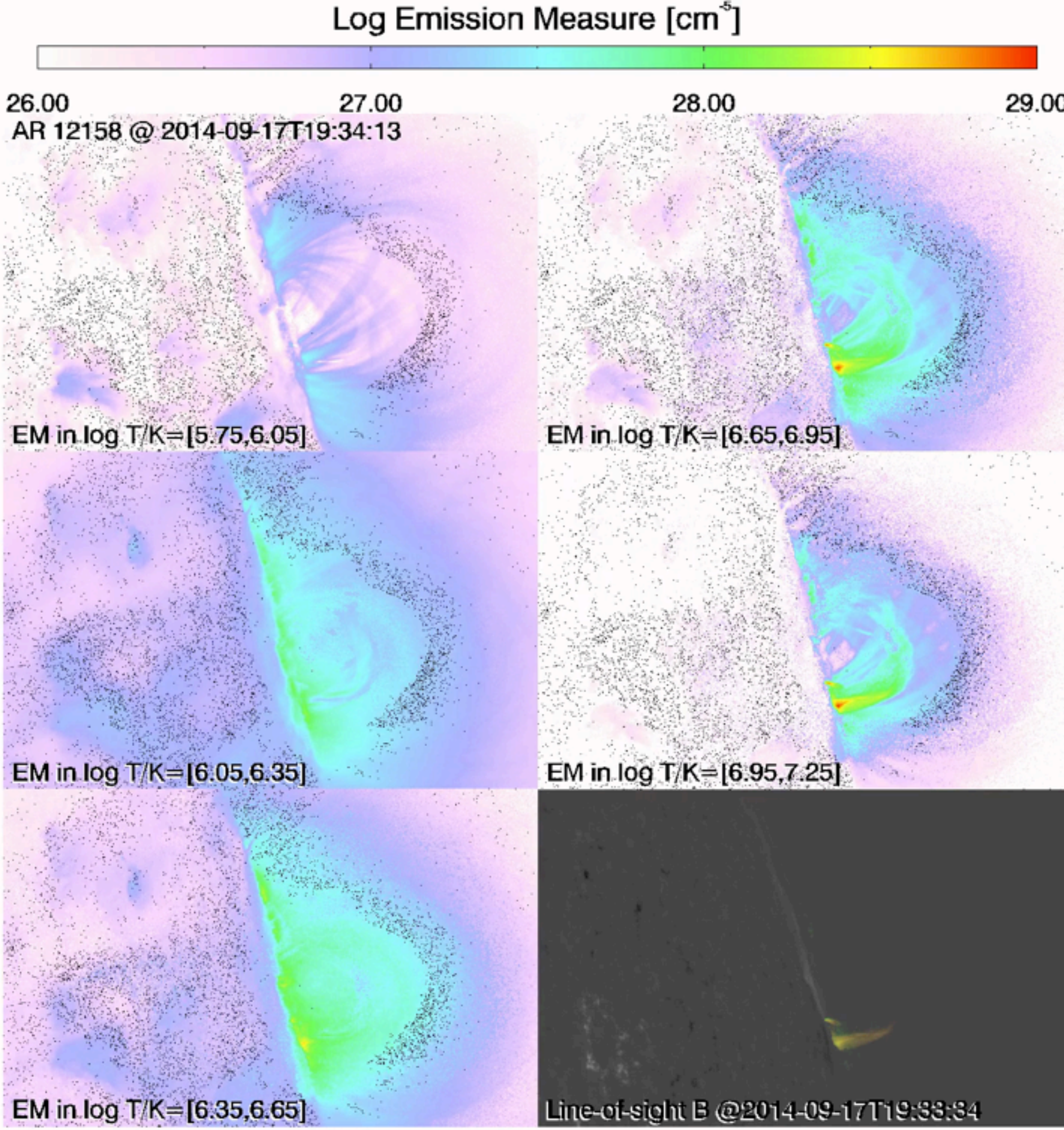

Other panels:

EM in various log T bins

- **Tell-tale signs of chromospheric evaporation**
- **Loops filled with plasma at 10 MK and above**
- **Loops cool to lower log T bins**
- **At time (~20:29 UT) when plasma cools down to log T/K ~ 5.8, coronal condensations in SJI 1330 begin to appear.**

Lower right panel only

Greyscale:

B_{los} from HMI

Green: 6MK EM

Yellow/Red: 10 MK EM

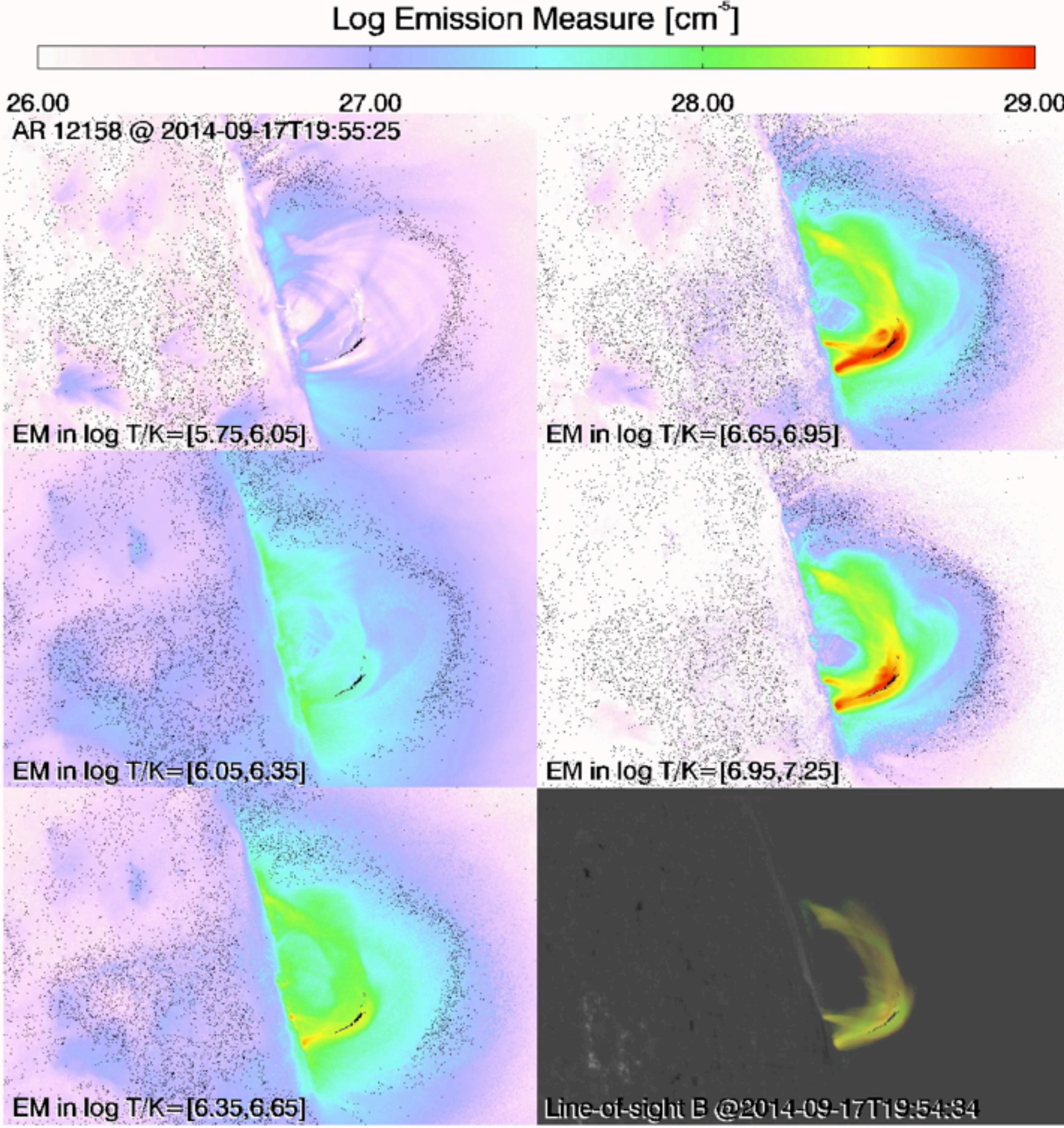

Other panels:
EM in various log T bins

- **Tell-tale signs of chromospheric evaporation**
- **Loops filled with plasma at 10 MK and above**
- **Loops cool to lower log T bins**
- **At time (~20:29 UT) when plasma cools down to log T/K ~ 5.8, coronal condensations in SJI 1330 begin to appear.**

Lower right panel only
Greyscale:
B_{los} from HMI
Yellow/Green: 6MK EM
Red: 10 MK EM

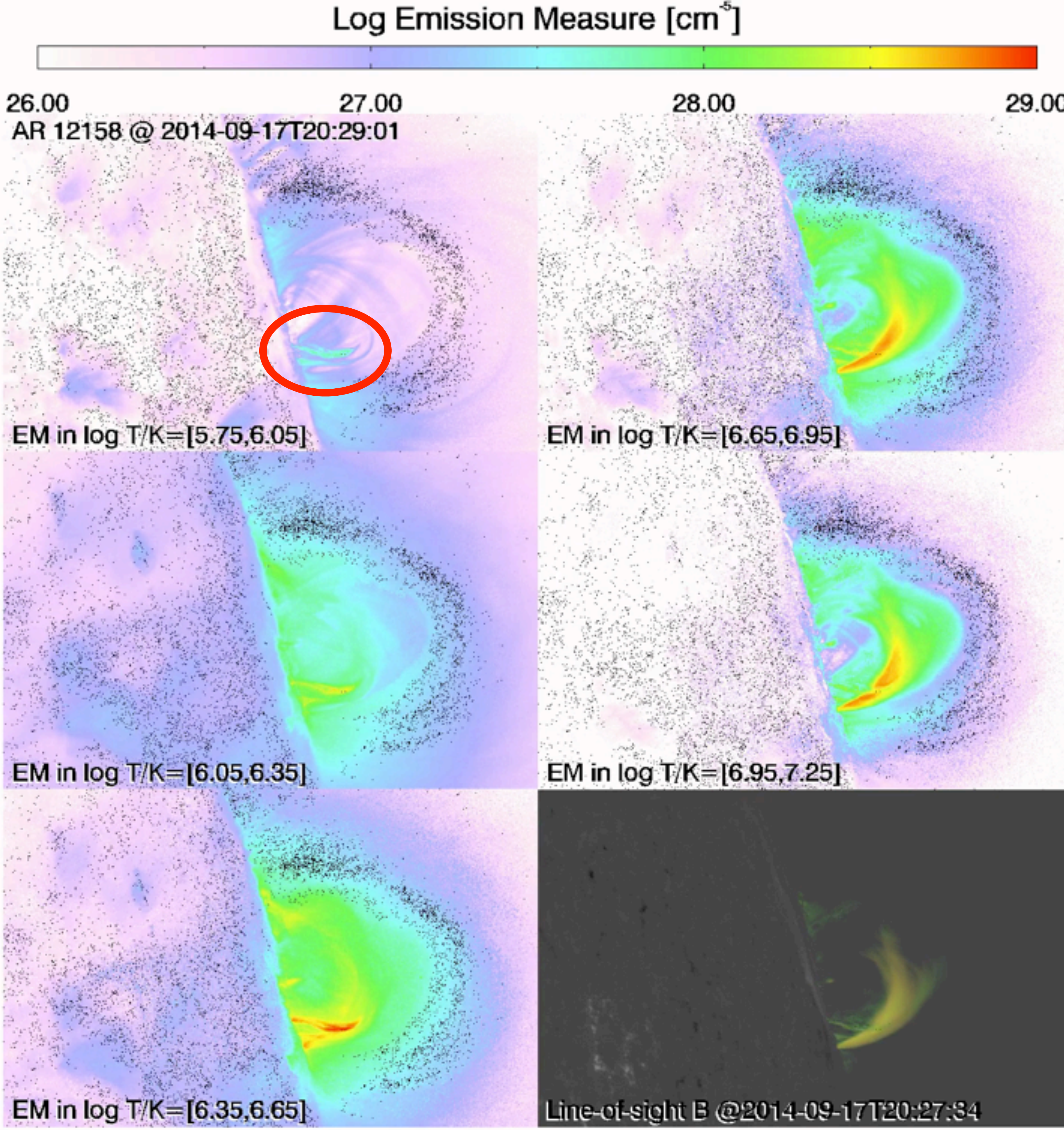

Other panels:
EM in various log T bins

- **Tell-tale signs of chromospheric evaporation**
- **Loops filled with plasma at 10 MK and above**
- **Loops cool to lower log T bins**
- **At time (~20:29 UT) when plasma cools down to log T/K ~ 5.8, coronal condensations in SJI 1330 begin to appear.**

Lower right panel only
Greyscale:
B_{los} from HMI
Yellow/Green: 6MK EM
Red: 10 MK EM

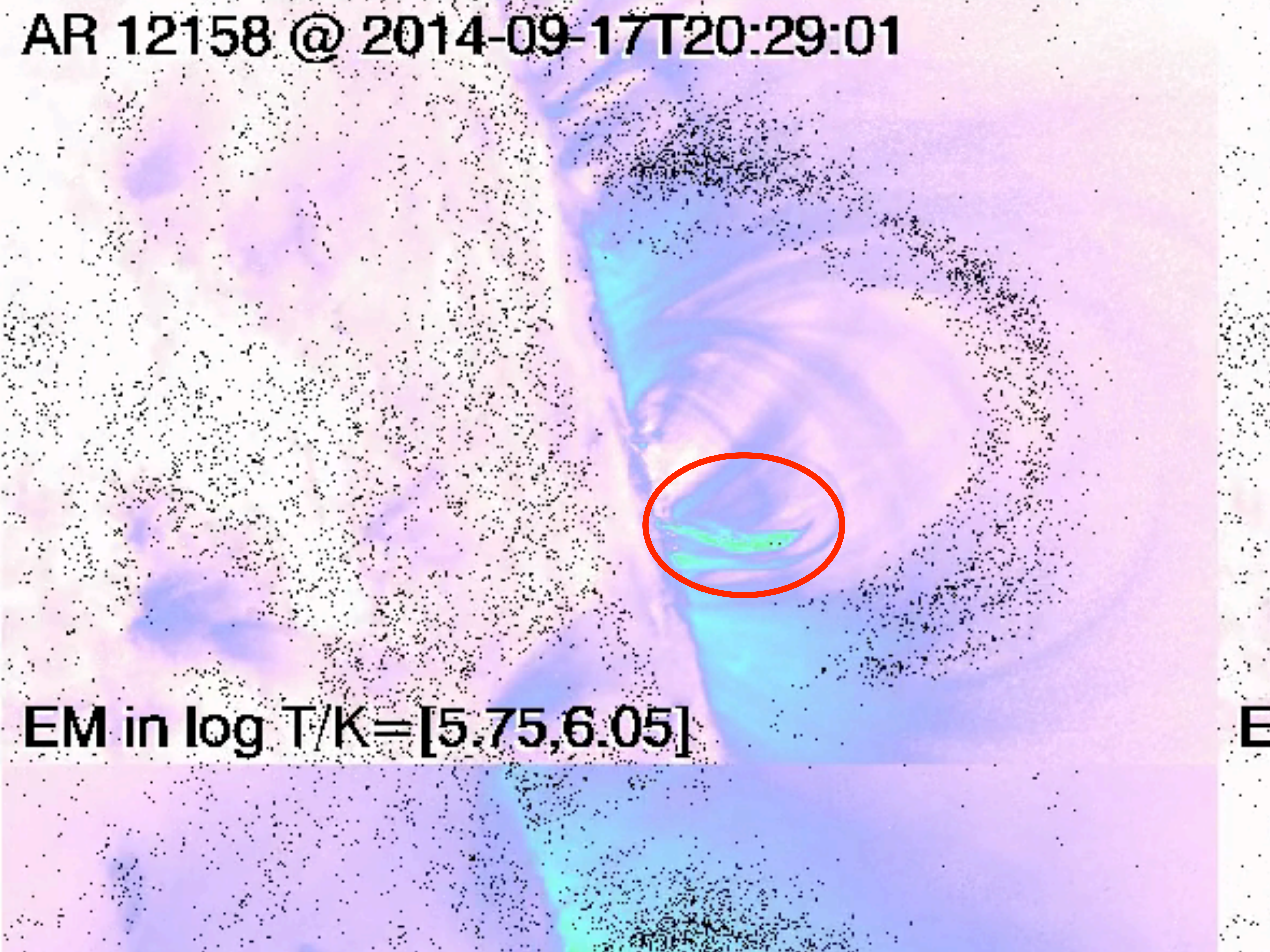
AR 12158 @ 2014-09-17T20:29:01
EM in log T/K=[5.75,6.05]

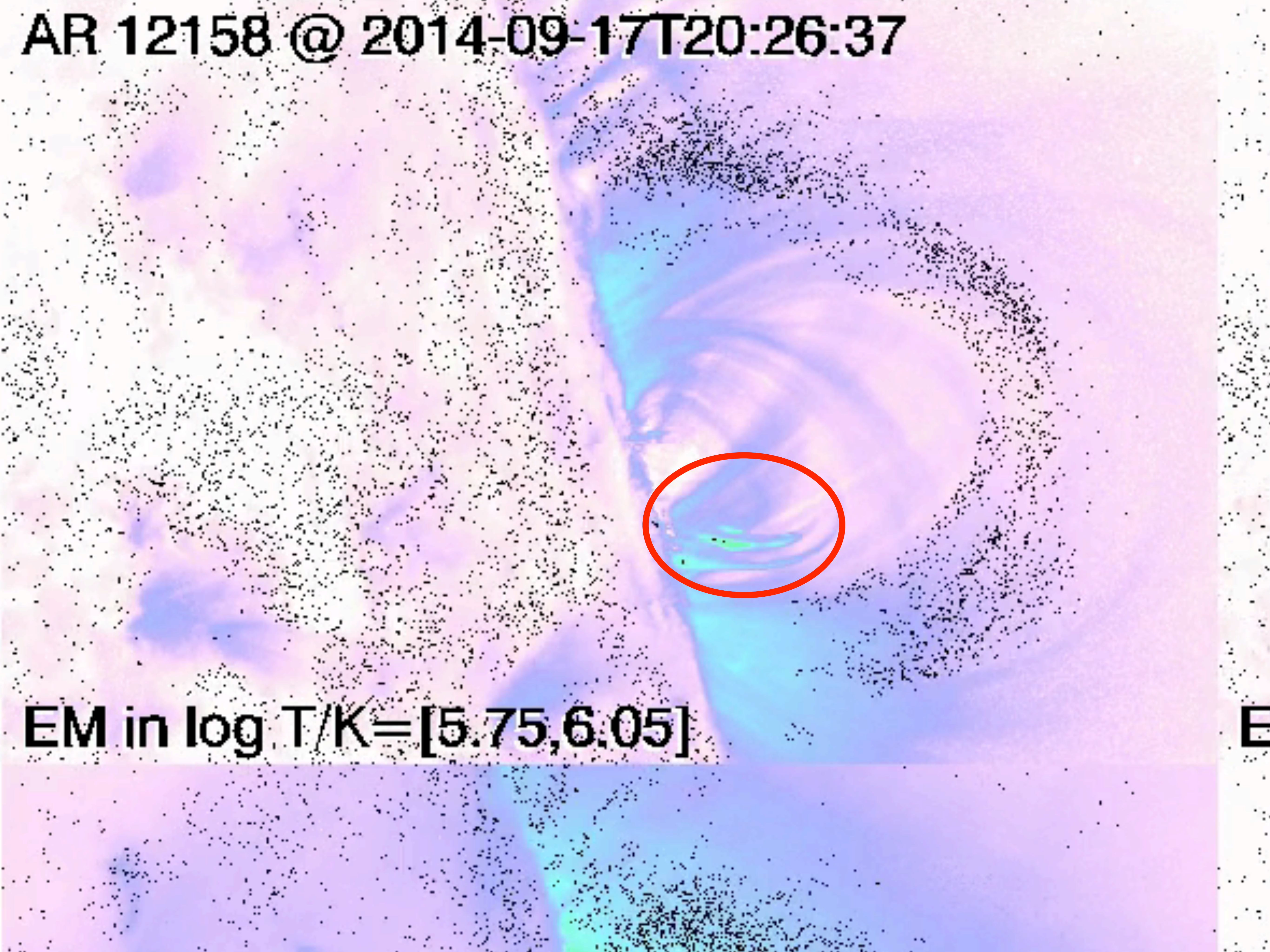
AR 12158 @ 2014-09-17T20:26:37
EM in log T/K=[5.75,6.05]

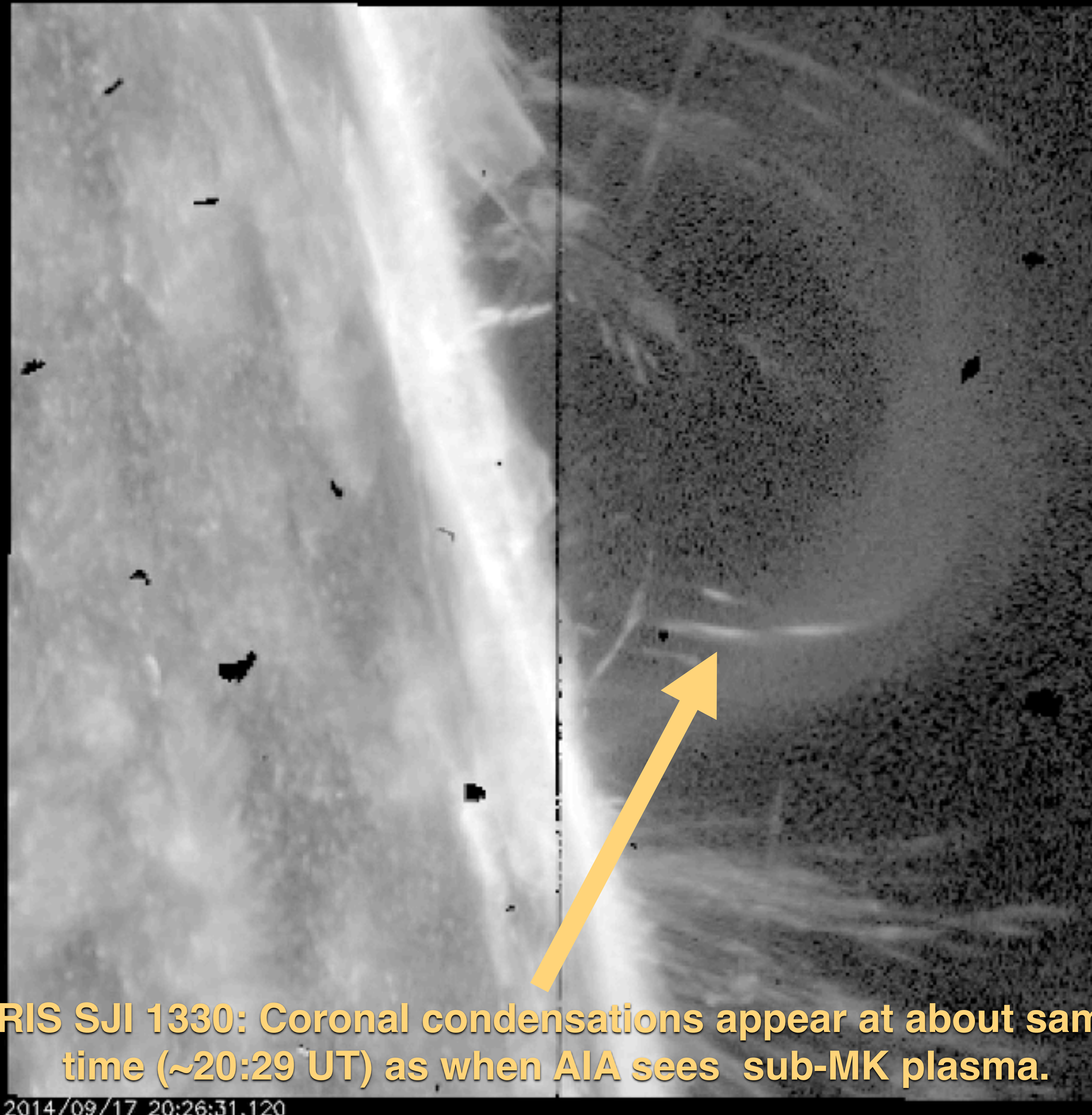

IRIS SJI 1330: Coronal condensations appear at about same time (~20:29 UT) as when AIA sees sub-MK plasma.